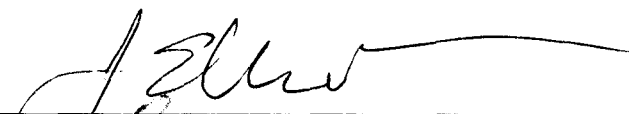# THE ACETYLCHOLINE BINDING PROTEIN OF *LYMNAEA STAGNALIS*

AS A BIOSENSOR AND A MODEL FOR LIGAND GATED ION CHANNEL

PROTEINS
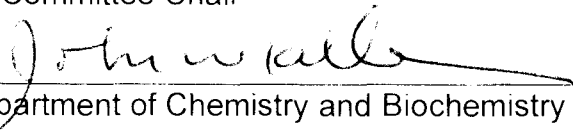
By

Abraham Edward Harms-Smyth

Recommended:

_____

_____

_____

_____
Advisory Committee Chair

_____
Chair, Department of Chemistry and Biochemistry

Approved:

_____
Dean, College of Natural Science and Mathematics

_____
Dean of the Graduate School

Dec 12, 2008

_____
Date

THE ACETYLCHOLINE BINDING PROTEIN OF *LYMNAEA STAGNALIS*

AS A BIOSENSOR AND MODEL FOR LIGAND GATED ION CHANNEL

PROTEINS

A

THESIS

Presented to the Faculty
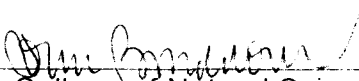
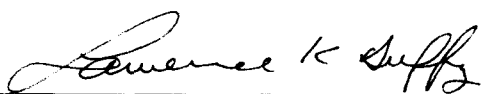of the University of Alaska Fairbanks

in Partial Fulfilment of the Requirements

for the Degree of

MASTER OF SCIENCE

By

Abraham Edward Harms-Smyth, B.S.

Fairbanks, Alaska

December 2008

Abstract

The structural similarity of the Acetylcholine Binding Protein (AChBP) from *Lymnaea stagnalis* to the extracellular ligand binding domain of Ligand Gated Ion Channel (LGIC) receptors suggests that the AChBP could be used to mimic cys-loop ligand-gated ion channel (LGIC) receptors. An LGIC mimic could be used as a sensor molecule in a range of biotechnology applications including high throughput drug screening as well as in vivo and in vitro sensing of biologically active compounds. It could also be used as a lead molecule for engineering novel proteins with binding characteristics similar to non-acetylcholine receptor LGIC's. The soluble AChBP is easily expressed and purified and can be produced in reasonably large amounts. This thesis explores the potential for using the AChBP and related proteins as biosensors by evaluating their action on three key medium and high throughput systems: Scintillation Proximity Assay (SPA), Surface Plasmon Resonance (SPR), and Microcantilevers (MC). As a preliminary step to developing a 5-HT$_3$R-ligand binding protein, by altering the ligand specificity of the AChBP, the interaction of 5-HT$_3$R ligands with the AChBP is also evaluated. The work presented in this thesis contributes to improved methods of drug design and testing, and to a better understanding of LGIC structure.

Table of Contents

List of Figures

List of Tables

Acknowledgements

I wish to give thanks to my friends/family, and committee. My advisor, Marvin Schulte, and his graduate students have been studying the 5HT$_3$R for a long time. My project is based on their work, and on the work of others: I am in their debt – whenever I say this or that amino acid is important to binding serotonin, or to binding this agonist or that antagonist, I owe them. These are my friends. Among them, I owe special thanks to Asha Suryanarayanan and Prasad Joshi. There are a great number of others, which I shall not list lest I forget one; everyone with whom I worked over these last few years, both as a teacher and a peer has my sincere thanks –they know who they are. My mentors include Rudy Candler, Roseann Leiner, Tom Green, Richard Stoltzberg, David Newman, Tom Clausen, Jestina Kusina, Bill Simpson, Kelly Drew, and Tom Kuhn. For my family, I realize that knowing that one of us succeeded as I have is thanks enough; but having them for a family is better by far than all of the success in the world. Of my family, Mom, Tran, Sarah, Sheila Chapin, Anshul and Maegan have been particularly critical to my success at this odd endeavor. My grandmother, Kathleen Smyth, insured that I would finish college. Glenn Herring was the first to call me "professor." My committee members, Jocelyn Krebs, Mike Harris, and George Happ, are wonderful people and great scientists; it is a great honor to have answered to them. Thanks to John Keller and the rest at UAF Chemistry and Biochemistry, and the Graduate School for very helpful edits. Thanks to those who suffer from the diseases, disorders and exceptionalities we work on treating and understanding, for it is they who make our work meaningful. Above all, I want to thank God for lending me this universe for this incredible journey.

Chapter 1: Introduction.

1.1   Ion Channels and Communication between Cells.

Living cells are surrounded by membranes. These membranes must be flexible, self-sealing, and selectively permeable, to allow for movement, cell replication, and interaction of the cell with its environment [1]. Selective permeability must also allow for molecular communication between cells in order to permit cooperation in multi-cellular organisms. In more complex organisms, one cell can regulate the physiology of another through the release of peptides, proteins or small ligands.

This ability to regulate, and be regulated by, other cells, frequently requires the release of a molecule (a ligand), or group of molecules, capable of interacting with proteins on the target cell. The system thus involves release of a ligand and its subsequent interaction with a receptor protein. Receptor systems are extremely diverse, often complex and always well regulated. Ligand Gated ion channel systems are conceptually simple in mechanism; a messenger molecule (ligand) from the first cell interacts with a channel protein (receptor) on the second cell. The ligand induces or stabilizes an open channel conformation in the receptor protein that allows an inward or outward movement of ions.

The ability of ions to carry a charge (thus altering the electrical potential of a cell) and to bind and regulate intracellular proteins and nucleic acids makes them ideal molecules for inducing physiological changes in cells; thus much of the communication between cells is carried out via "ligand-gated" ion channels, also known as "ionotropic receptors." Ion channel mediated cell-cell communication is fast and therefore well suited to coordinating cellular activity in the nervous systems of complex organisms. Ion channels are typically divided into ligand-gated and voltage gated. This thesis focuses on the pentameric cys-loop superfamily of ligand-gated ion channel proteins (LGIC). Other LGIC

families include NMDA-type, kainate-type, and AMPA-type tetrameric glutamate-gated cation channels, and trimeric ATP-gated channels [2].

1.2 The cys-loop Ligand Gated Ion Channel (LGIC) Superfamily.

The cys-loop LGIC superfamily of receptors are typified by a characteristic disulfide bond between two conserved cysteine residues 13 amino acids apart in the primary sequence of all subunits. Mutation of these cysteines and elimination of this disulfide bond renders the protein non-functional. Cys-loop LGIC proteins display a pentameric quaternary structure and can be either homomeric or heteromeric (figure 1.1). Individual subunits are characterized by a large extracellular amino-terminal domain and four transmembrane (TM) regions (M1, M2, M3, and M4). The extracellular domain is dominated by a large pre-M1, NH_3 domain, a small M2-M3 region and a few C-terminal residues. The intracellular domain contains a small M1-M2 region as well as a larger M3-M4 region.
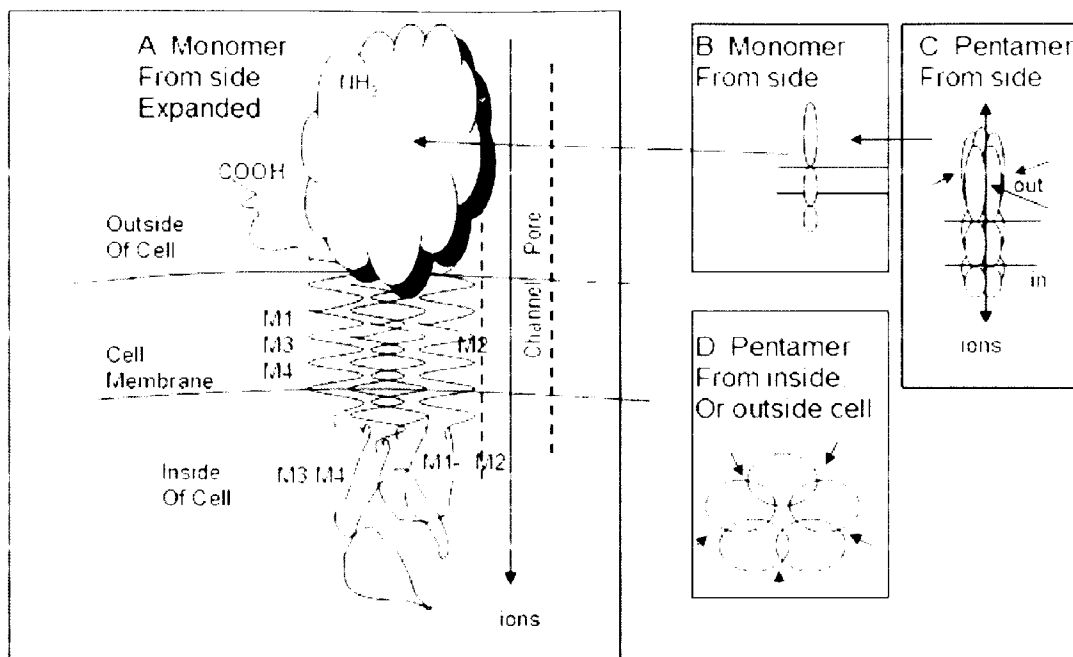
Figure 1.1: Schematic of Cys-loop LGIC. A: Side views of single subunit (the other four subunits are omitted for clarity). B, C, D: Side and top (outside cell) views of the pentamer. In a homomeric receptor, each of the five subunits forming the pentamer are identical; in a heteromer, the pentamers are formed of more than one different subunit type, but the overall structure remains similar. Arrows in C and D indicate potential ligand-binding sites. See text for further explanation.

1.3   Neurotransmitter Binding Site of LGIC's.

The agonist binding site in cys-loop receptors is located at the interface between the extracellular amino-terminal domains of two adjacent subunits. Five potential binding sites exist in the pentameric receptor with each subunit forming an interface with two other subunits. In homomeric receptors all 5 interfaces likely function as agonist binding sites. In heteromeric receptors 2-3 agonist binding sites are typical. The remaining interfaces may function as binding sites for allosteric modulators in some receptors. Binding sites are composed of six "loops" of amino acids commonly referred to as A-F (Figure 1.2). Each subunit contributes three loops on each of its two interfaces with loops A-C located on one interface (the + face) and D-F located on the other interface (the − face).
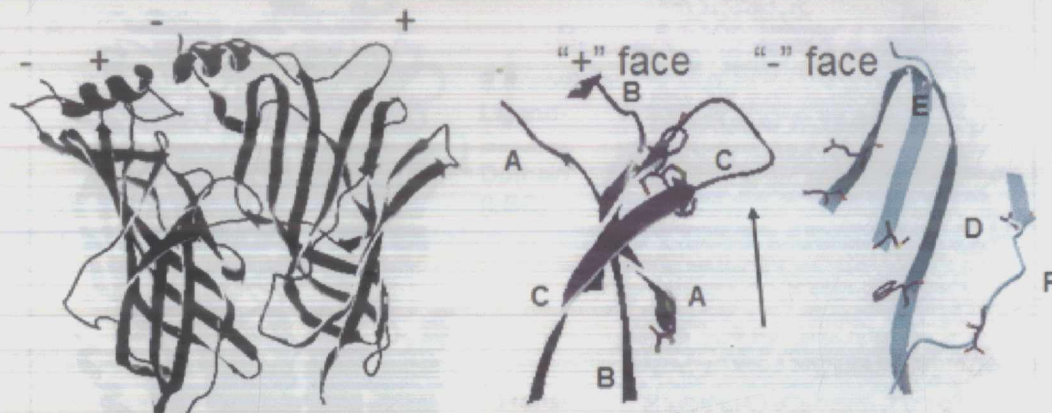
Figure 1.2: Principal Binding Loops of LGIC Receptors. Left: The relative orientation of the binding domains (NH$_3$-terminals) of two LGIC subunits. Middle and right: the plus (+) and minus (-) faces (respectively), separated horizontally (i.e. expanded), with their corresponding loops labelled. A, B, and C loops are labelled twice in order to clarify their positions. The ligand inserts in the vicinity of the arrow, partly under the C-loop, and against the B loop and possibly the A-loop on the plus face and probably the D, E, and possibly F loops on the minus face. Protein Data Bank file 1I9B (AChBP [3]) and DeepView Swiss Pdb Viewer version 3.7 were used to create this figure.

The key binding site regions of Cys-loop LGIC's were identified by affinity labelling studies of the muscle nicotinic acetylcholine receptor, the prototypical cys-loop LGIC [4]. Structurally homologous binding loops have been identified in all members of the cys-loop LGIC superfamily. The specific involvement of particular amino acids within the loops has been investigated using a multitude of techniques including affinity labelling, alanine scanning mutagenesis, substituted-cysteine accessibility method (SCAM), and others. In addition to binding site structures, the quaternary structure of the nicotinic acetylcholine receptor has also been derived from electron diffraction studies of nicotinic receptors obtained from the torpedo electric fish [5]. The most current and detailed model of the torpedo nAChR is shown in Figure 1.3. An excellent review of binding site structure of the prototypical nAChR can be found in Hogg et al [4].

A.

B.

Extracellular
Ligand-
Binding
Domain
(LBD)

Trans-
Membrane
(TM)

C.

D.
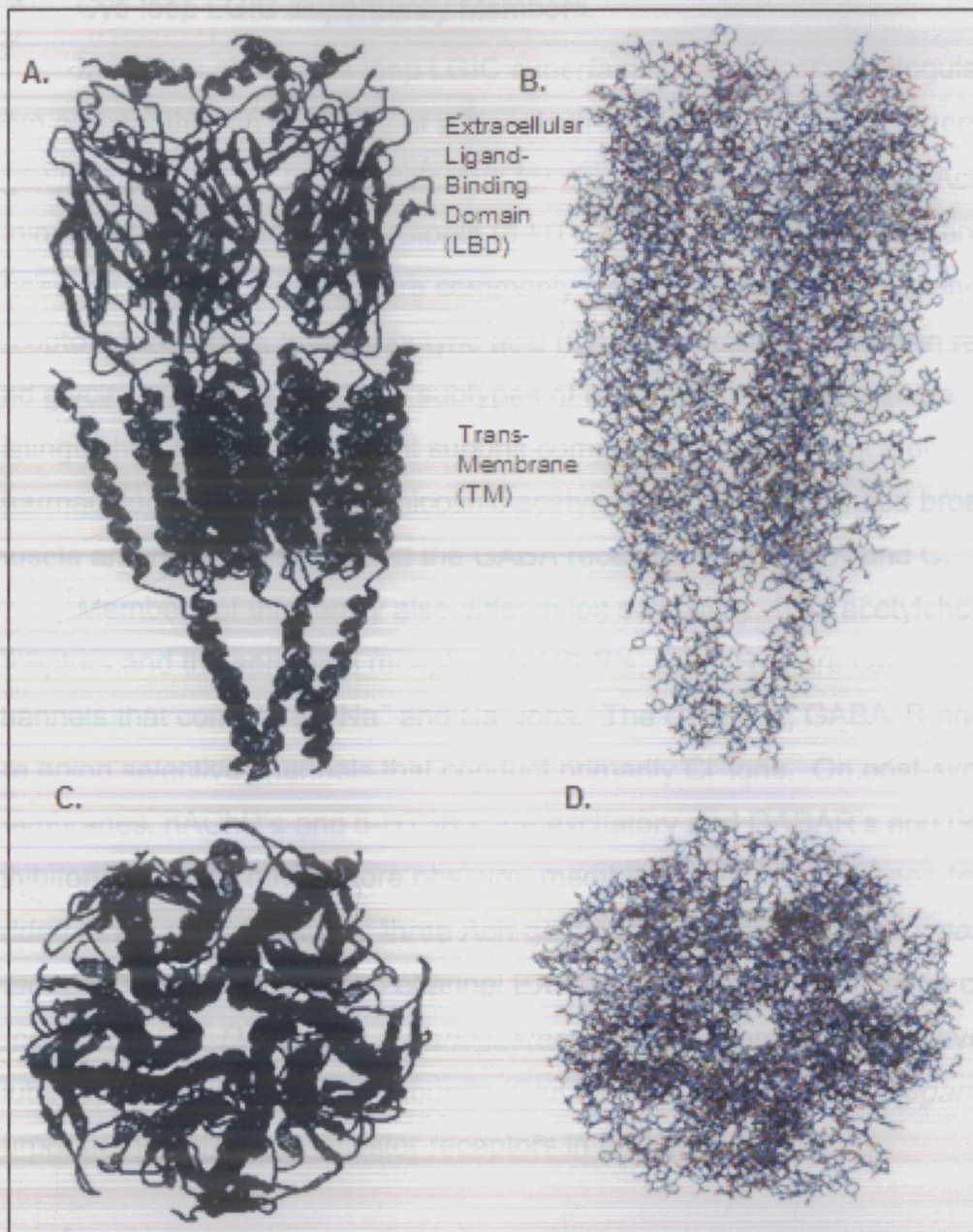
Figure 1.3: Torpedo nicotinic acetylcholine receptor structure. A, B: Ribbon and atomic structures, as viewed from side. C, D: Ribbon and atomic structures, as viewed from top (outside of cell). Protein Data Bank (PDB) file 2BG9 [5], images created using the DeepView/ Swiss Pdb Viewer 3.7.

1.4   Cys-loop LGIC Superfamily Members.

Members of the Cys-loop LGIC superfamily are typically distinguished from one another on the basis of their selectivity for a particular endogenous agonist (figure 1.4).   LGIC's selective for nicotine and acetylcholine (Ach), γ-aminobutyric acid (GABA), serotonin (5-HT), and glycine have been identified. These ion channel receptors are commonly referred to as nicotinic acetylcholine receptors (nAChR's), γ-aminobutyric acid (GABA) receptors, serotonin receptors, and glycine receptors. Multiple subtypes of each receptor class can be distinguished based on different subunit compositions that produce distinct pharmacological profiles. The nicotinic acetylcholine class is divided broadly into muscle and neuronal types and the GABA receptor into types A and C.

Members of this family also differ in ion selectivity. The acetylcholine receptors and the serotonin receptors (nAChR's, 5-HT$_3$R's) are cation selective channels that conduct K^+, Na^+ and Ca^+ ions. The GABA$_A$R, GABA$_C$R and GlyR's are anion selective channels that conduct primarily Cl$^-$ ions. On post-synaptic membranes, nAChR's and 5-HT3R's are excitatory and GABAR's and GlyR's are inhibitory. Several other, more obscure, members have recently been tentatively added to the superfamily [2]: three Ach-gated Cl$^-$ channels from *Lymnaea stagnalis,* GABA-gated cation channel EXP-1R, a Zn^{2+} activated cation channel receptor (ZACR, *Drosophila melanogaster* eye), two avermectin-sensitive glutamate-gated Cl$^-$ channel subunits (GluClR, in *Caenorhabditis elegans*), and purported homologous ancestor receptors in prokaryotes [2].
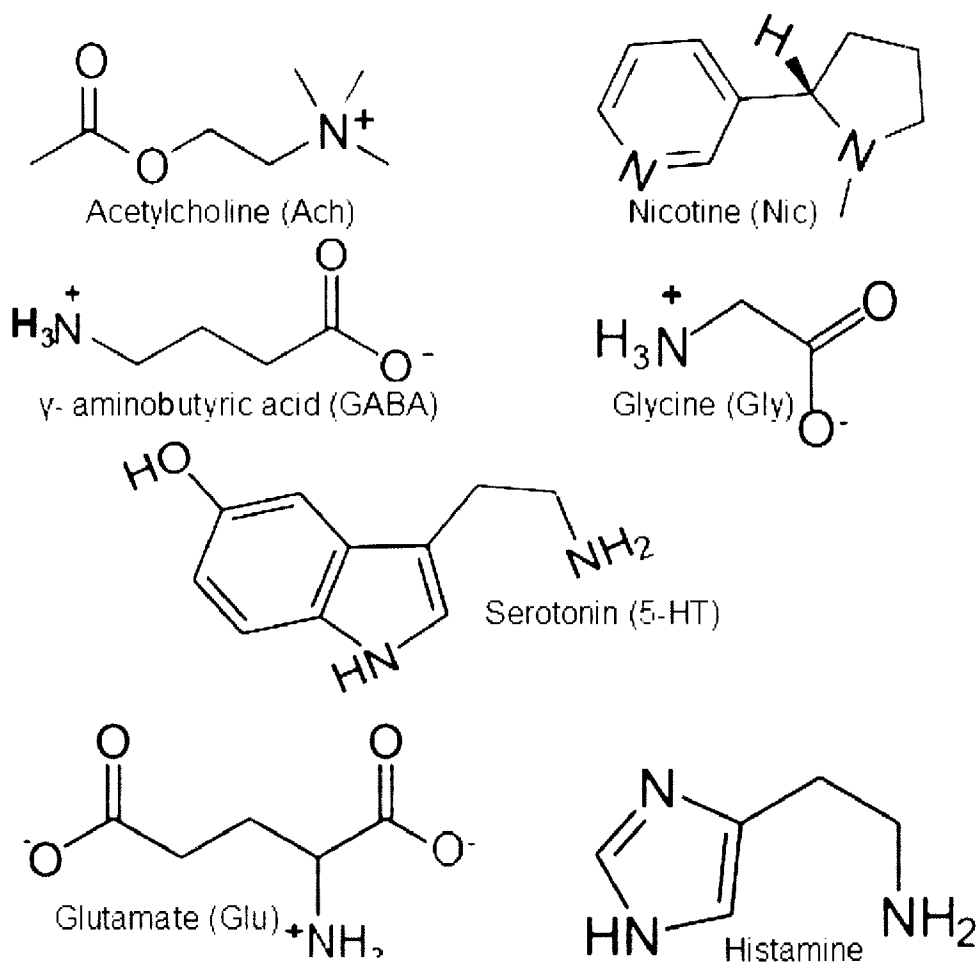
Figure 1.4: Structures of endogenous agonists for known Cys-loop LGIC. Acetylcholine and serotonin are the primary neurotransmitters for excitatory nAChR's and 5-HT$_3$R's, respectively. Nicotine is a partial agonist at nAChR's. Inhibitory neurotransmitters glycine and GABA are also shown, as well as histamine and glutamate, which activate newly discovered LGIC.

1.5   Cys-loop LGIC physiological implications.

Cys-loop receptors are apparently involved in many physiological processes including learning and memory, regulation of blood flow, fluid balance, gastric motility, appetite control, and pain [2]. Multiple disease states are thought to involve LGIC's including Parkinson's disease (PD), schizophrenia, Alzheimer's disease (AD) [6-8], autism spectrum disorders [9], attention deficit- hyperactivity disorder (ADHD) [6], and nicotine (cigarette smoking) and alcohol addiction [10].

Despite enormous efforts on the part of a large number of researchers, the precise role of LGIC receptors in these many of these disorders remains unclear.

As important receptors implicated in human disease, the cys-loop LGIC superfamily of proteins present attractive drug targets. Antagonists, agonists and allosteric modulators are all potentially useful therapeutic agents. For example transdermal nicotine has been shown to increase attention in AD and ADHD patients, and to act on the amygdalae and hippocampus in rat models [6]. Benzodiazepines are commonly used to treat seizure disorders by increasing activity of GABA receptors in the central nervous system (CNS) [2]. Serotonin antagonists are used to treat chemotherapy induced emesis and nicotinic receptor modulators such as galanthamine are being tested as cognitive enhancers in AD patients. Steroids and anaesthetics are also thought to alter LGIC receptor function. An incomplete knowledge of the specific receptor type and subtypes involved in particular disease states presents problems in developing therapeutic approaches to neurological disorders involving LGIC receptors. This type of evaluation requires subtype selective drugs that are often unavailable. The issue is complicated by the sometimes broad selectivity of LGIC receptors by even endogenous agonists. For example it is known that nAChR's are modulated by serotonin. This "crosstalk" between receptors makes it difficult to identify which neurotransmitter is involved.

Developing more subtype selective compounds is hindered by an incomplete knowledge of the drug/receptor interaction at the molecular level and the inability to rapidly evaluate drug candidates on multiple receptors subtypes.

1.6 Serotonin type 3 receptor (5-HT₃R) subtypes.

The serotonin type 3 receptor (5-HT$_3$R) was first discovered in 1957 by Gaddum and Picarelli who observed the effects of serotonin on guinea pig ileum [11]. Originally named the "M receptor" this discovery represented the first identification of a receptor for serotonin. In 1989, [12] this receptor was

determined to be a LGIC and was re-named the 5-HT type 3 receptor. Other serotonin receptors including types 1, 2 and 4 are not members of the LGIC receptor family but are considered "metabotropic" or G-protein coupled receptors. Genes codling for A, B, C and E subunits of the Serotonin type 3 receptor have been identified [13], [14]. A gene coding for a D subunit has also been identified but lacks the amino terminal (extracellular) region. The pharmacology of 5-HT_3Rs was quickly found to vary between species and evidence for different subtypes within a single species was first noted by Bonhaus et al in 1993 who observed differences between responses in mouse ileum and cortex [15]. Early data suggested that $5HT_3R$ subunit A formed homomeric receptors and this was thought to be the predominant subtype in both central and peripheral tissues. With the cloning of the B subunit in 1999 [16] it became clear the 5-HT_3Rs also express heteromeric 3A-3B receptors; this finding was assumed to account for the findings of Bonhaus [15], since the heteromeric 3A-3B receptors were found in the ileum, while homomeric 3A receptors were found in the cortex. The precise stoichiometry of the heteromeric receptors is unknown but has been postulated that AB receptors are composed of two A subunits and three 3B subunits. Ligands that could distinguish between different subtypes were unavailable until the discovery of picrotoxin in 2003 [17].

As recently as 2003, Van Hooft [18] argued that there may be only homomeric 3A receptors in the central nervous system (CNS). In fact, only the short form of the 3A receptor was known in the CNS of humans. As a consequence researchers focused on the pharmacology and function of the homomeric 5-$HT_{3A}R$. However, recent studies show that the 3B-subunit is also expressed in the human hippocampus [19], and transcribed in other areas of the brain, in amounts even higher than the 3A transcription, with a few different splice variants [20]. The solution to the problem of receptor heterogeneity and localization is quite important, as it is a prerequisite for adequately understanding 5-HT_3R involvement in the normal physiology of the CNS and its role in disease.

While localization of individual subunits is amenable to immunohistochemical methods, determination of subunit composition of individual receptor is more difficult. This analysis will likely require new ligands that discriminate between different heteromeric and homomeric subtypes of the 5-HT$_3$R in addition to single channel analysis. The development of new, subtype selective, pharmacological agents for the 5-HT$_3$R family is critical to determining its distribution and role in disease.

1.7   The 5-HT$_3$R primary binding site.

Site-directed mutagenesis studies on the murine (mouse) 5-HT$_{3A}$R have identified a number of amino acid residues are important to binding agonists and competitive antagonists to the 5-HT$_3$R [21]. Site directed mutagenesis studies have focused on regions of the 5-HT$_3$R amino terminal homologous to the nAChR binding loops A-F (recall figure 1.2 above). Key amino acids have been identified in loop B [22], loop C [23] and loop E [24] of the short splice variant of the murine type A 5HT$_3$R. Figure 1.5 shows the positions of these loops and some of the important residues, according to one model, which is based on the AChBP discussed in the next section and throughout this work.
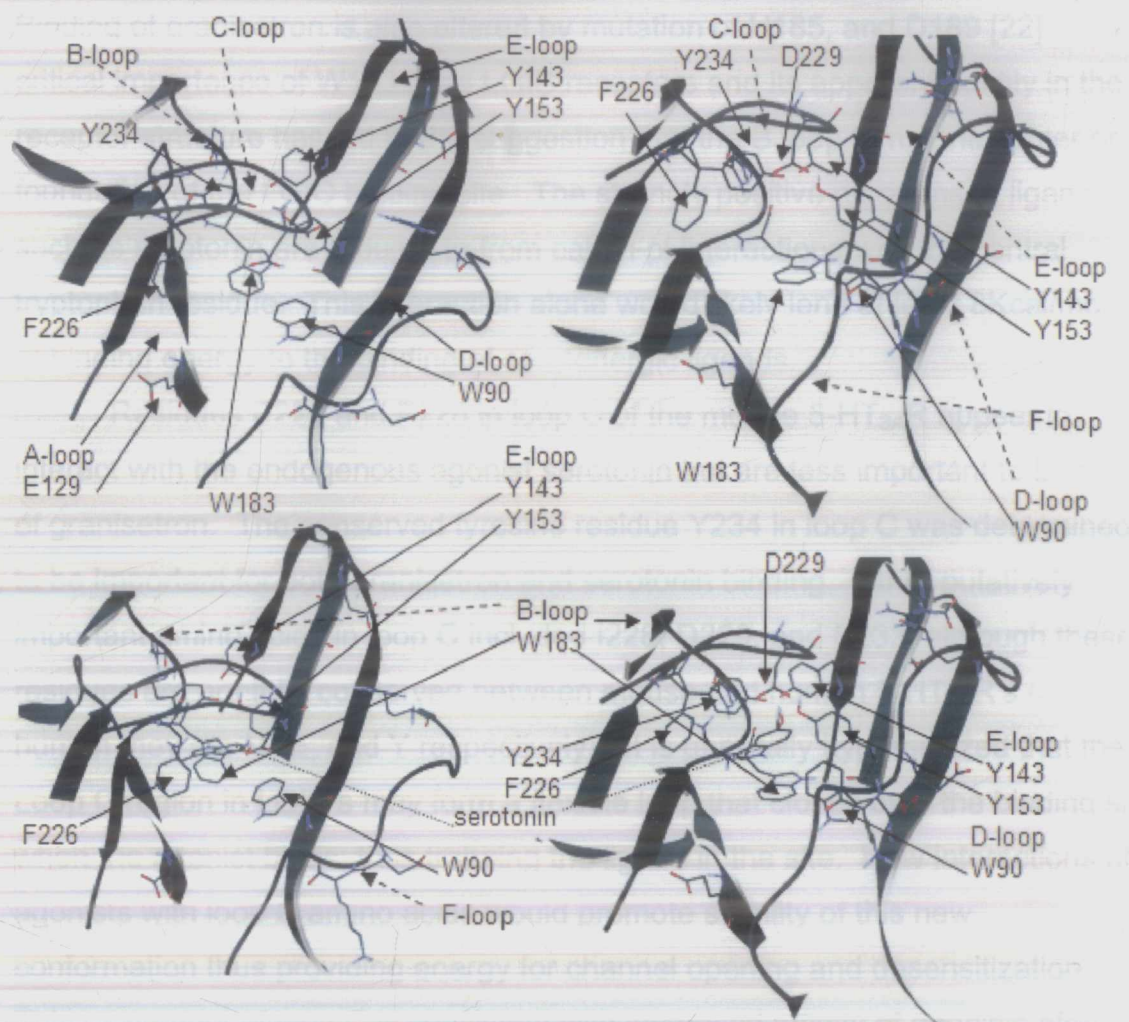
Figure 1.5: Structure of the binding site of the 5-HT₃R. Top and bottom left are views from the side of the receptor. The ligand serotonin (5-HT) is inserted on the bottom figures. Top and bottom right are views of the binding site rotated into the plane of the page; that is, viewed from the membrane side. Solid arrows indicate positions of residues as labelled, dashed arrows indicate the position of loops; in the bottom figures, dotted lines indicate the position of serotonin. Atoms are coloured as follows: Oxygen red, nitrogen dark blue, carbon black, hydrogen light blue. Figure was created using Protein Data Bank file 1I9B (AChBP [3]) and DeepView Swiss Pdb Viewer version 3.7.

In the loop B region, binding of the 5-HT₃R antagonist granisetron appears to involve W183 (conserved in most cys-loop receptors). Mutation of W183 to Y, F or A (standard one-letter amino acid abbreviations [1] are used throughout this thesis) severely alters binding of all competitive ligands including serotonin.

Binding of granisetron is also altered by mutation of H185, and D189 [22]. The critical importance of W183 in all LGIC receptors and its apparent rigidity in the receptor structure has led to the suggestion that the B loop forms the center or foundation of the LGIC binding site. The strongly positive nitrogens of ligands such as serotonin are thought to from cation-pi interactions with the central tryptophan residue. This interaction alone would likely lend at least 8Kcal/mole of binding energy to the binding of serotonergic ligands.

Residues E225 and F226 in loop C of the murine $5\text{-HT}_{3A}R$ appear to interact with the endogenous agonist serotonin but are less important to binding of granisetron. The conserved tyrosine residue Y234 in loop C was determined to be important for both granisetron and serotonin binding. Other putatively important amino acids in loop C included I228, D229, and S233, although these residues are not fully conserved between mouse and human $5\text{-HT}_{3A}R$'s (in the human they are M, E, and Y respectively). It is generally hypothesized that the Loop C region in LGIC's may form a flexible loop that closes over the binding site when the agonist binds; thus trapping the ligand in the site. New interactions of agonists with loop C amino acids would promote stability of this new conformation thus providing energy for channel opening and desensitization. This movement of loop C is consistent with increased affinity of agonists after channel opening. Antagonists are thought to be too large to allow this conformational change and do not appear to interact extensively with loop C amino acids.

In loop E, two tyrosines (Y143 and Y153, also sometimes called Y142 and Y152, respectively) were found to be important to binding of several agonists including serotonin and m-chlorophenylbiguanide (mCPBG) - a partial agonist. These residues did not substantially alter binding of granisetron but did affect binding of the newly discovered antagonist lerisetron. Lerisetron represents a new structural class of 5-HT_3R antagonists and would thus likely interact slightly different with the 5-HT_3R binding site. While it is unclear exactly what role the E

loop plays in the 5-HT$_3$R, it seems likely that it becomes more important to binding of agonists as the channel changes conformation to the open and desensitized states. This conformational change may involve a movement of the E-loop on the − face of the binding site towards the + face. Similar to the C-loop this would lead to increased binding energy for agonists and provide energy for channel opening.

Other residues known to be important are the conserved W90 in the D-loop, and E129 in the A-loop [2]. A more complete analysis of this topic is given in chapter 4.

1.8 Acetylcholine-binding protein (AChBP).

The AChBP (figure 1.6) was originally discovered in the great pond snail, *Lymnaea stagnalis*. Two additional homologues of this protein have also been identified in the sea hare *Aplysia californica* [25] and freshwater snail *Bulinus truncatus* [26]. In these gastropod molluscs this protein is thought to be secreted by glia and its presumed role is to regulate synaptic function through binding and sequestering of acetylcholine; but it is possible that it could have other functions as well, such as defending the organism against toxins. Sequence analysis suggests that this protein may have evolved as a result of a truncation of the nAChR in ancestral snails.
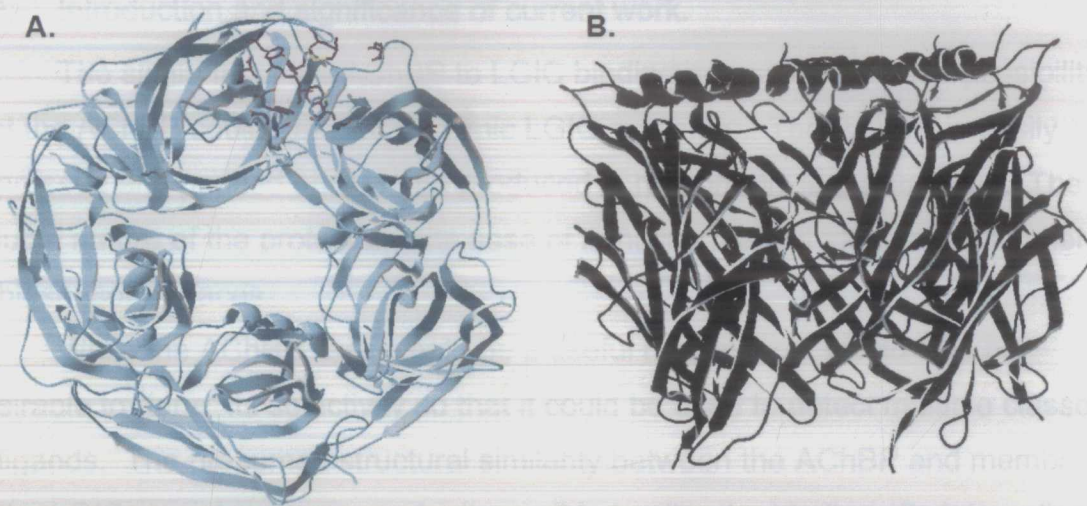
Figure 1.6: AChBP pentamer. A: bottom view. B: side view. From Protein Data Bank (PDB) file 1I9B, [3], visualized using DeepView Swiss Pdb Viewer version 3.7.

The acetylcholine-binding protein (AChBP) [3, 27] has been used extensively in developing homology-based computer models of the N-terminal binding domains of cys-loop ligand gated ion channels (LGIC's) [22, 23, 28-33]. The AChBP is thought to be structurally homologous to the amino terminal region of LGIC receptors based on the reasonably high sequence identity between these proteins (15-30%). Since it is a soluble protein, the AChBP has been crystallized and its structure determined to a resolution of 1.8Å. The AChBP displays a pentameric quaternary structure very similar to the N-terminal domain of the nAChR determined from electron diffractions studies [5, 27]. In addition, amino acids within the binding site loops identified by affinity labelling and site directed mutagenesis on the nAChR correspond to amino acids located in the AChBP binding site. The combination of sequence homology, similarities in overall structure and location of loop regions suggests that the AChBP can be used to develop reasonably good models of LGIC binding sites.

1.9   Introduction and significance of current work.

The similarity of the AChBP to LGIC binding domains raises the possibility that the AChBP could be used to mimic LGIC receptors. The AChBP is easily expressed and purified and can be produced in reasonably large amounts. The soluble nature of the protein and its ease of handling make it ideal for attachment to biosensor surfaces.

While the AChBP itself would be a useful biosensor, it would also be desirable to "tune" its selectivity so that it could be used to detect multiple classes of ligands. The presumed structural similarity between the AChBP and members of the LGIC superfamily may make it possible to alter the binding site interactions via site-directed mutagenesis and change the selectivity of the AChBP to favour 5-HT$_3$R ligands over nicotinic ligands. This approach will require detailed understanding of the interaction of ligands with both the target receptor (such as the 5-HT$_3$R) and the AChBP. Models of interaction for different LGIC receptors and the comparative pharmacology of receptors ligands are available although more refinement may be necessary. Numerous mutagenic studies can provide the necessary information to begin mutating the AChBP. Pharmacological data of the AChBP itself is more limited.

1.9.1   AChBP pharmacology.

While the AChBP appears to be a good model for LGIC receptors and homology models based on this protein are available for nicotinic, GABA, Glycine and serotonin receptors, very little is known about the pharmacological selectivity of the AChBP. For example, while several labs have constructed homology models of the 5-HT$_3$R and used these models to model the interaction of granisetron, lerisetron, d-tubocurare, serotonin and m-chlorophenylbiguanide with this receptor, no comparative pharmacology has been done to determine the interaction of these compounds with the AChBP itself. Without pharmacological

data for LGIC ligand interactions with the AChBP, any analysis of the quality of the docked homology model is flawed. To make matters worse, it generally appears to be assumed that AChBP pharmacology will mimic the nAChR and is unlikely to bind 5-HT$_3$R ligands with any great affinity. This is an invalid assumption that may lead to incorrect binding models for 5-HT$_3$Rs. Better pharmacology data for the AChBP would help distinguish between competing models of ligand/receptor interaction and improved homology models of these receptors. Better models of LGIC along with a comprehensive pharmacology of the AChBP can be used as a basis for protein engineering of the AChBP as a broad use sensor molecule.

1.10 Study Hypotheses and Objectives:

The overarching goal of this project is to use the AChBP as a lead molecule for the development of high throughput biosensor devices. This goal rests on two fundamental hypotheses:

1. *The AChBP can be attached to biosensor surfaces and trigger a response that can selectively detect the presence and affinity of nicotinic ligands.*

> **Objective 1.1: Develop an expression and purification scheme** for the AChBP that permits rapid purification of sufficient quantities of protein.

> **Objective 1.2: Determine the storage qualities of the AChBP** in solution and identify ways of stably storing the protein over a long time period (months).

> **Objective 1.3: Determine the functionality** of the receptor on three biosensor platforms – Surface Plasmon Resonance, Scintillation Proximity Assay and Microcantilevers.

Objective 1.4: Determine the sensitivity and stability of the AChBP on each of the platforms tested in Objective 1.3.

2. The AChBP can be engineered to selectively recognize different classes of LGIC by mutating key binding site amino acids in the AChBP to corresponding amino acids of the target LGIC receptor.

Objective 2.1: Conduct pharmacological studies of the AChBP to determine the affinity of a broad range of LGIC ligands with the AChBP in its native form

Objective 2.2: Construct point mutations based on predictions from homology modelling and ligand studies of the binding domain of the serotonin type 3 receptor, which will increase affinity of serotonergic ligand and decrease affinity of nicotinic ligands (i.e. Alter the selectivity of the protein to one similar to the 5-HT$_3$R.).

Objective 2.3: Using information obtained as a result of Objective 2.2, create additional Binding proteins aimed at mimicking selectivity of 5-HT$_3$R subtypes.
(Long term objective – not part of the current thesis).

Materials and methods utilized to accomplish these objectives are found in Chapter 2 of this thesis. Objectives 1.1-1.4 are addressed in Chapter 3 (*AChBP as a molecular biosensor*) and Objectives 2.1 and 2.2 are addressed in Chapter 4 (*Binding of serotonergic ligands to the AChBP*). Only limited data is presented (in supplementary material) for Objective 2.2. Objective 2.3 is a long term objective of the overall study and the project is not yet ready to address this point. Chapter 5 summarizes all efforts to date and indicates future directions and goals of the project.

Chapter 2: Materials and Methods.

2.1 Construction of AChBP-containing plasmid DNA.

AChBP cDNA identical in sequence to the molluscan snail *Lymnaea stagnalis* was commercially synthesized and inserted into a p3xFLAG-CMV-9 vector containing a C-terminal 6x Histidine region and an N-terminal p3-Flag epitope tag. The vector also contains a G418-resistant gene for selection of stable transfectants in mammalian cell lines. Synthesis and cloning was performed by GENEART (Regensburg, Germany).

2.2 Amplification of AChBP Plasmid DNA.

XL1-blue supercompetent *E. coli* cells were transformed with the AChBP/p3XFlag-CMV-9 DNA using a standard protocol and reagents provided by Stratagene. (Stratagene, Cedar Creek, TX, USA, catalogue #200236). Minor modifications to this protocol were made: The procedure was scaled down by 50%, and beta-mercaptoethanol was omitted. DNA was purified by Qiagen Maxi-prep (Qiagen, Maryland, USA), using Qiagen's protocol. DNA was verified by restriction digest followed by agarose electrophoresis.

2.3 Stable transfection of AChBP in Human Embryonic Kidney.

DNA prepared by Qiagen Maxi-prep was used to develop stably transfected HEK293 cell lines (Human embryonic kidney cells, ATCC) that actively secrete an intact AChBP. Development of stably transfected cell lines results in consistent production of AChBP protein, high yields (1 mg per litre media) and rapid purification using the 6X His nickel binding region or AntiFlag antibody.

2.3.1 Growth conditions for HEK 293 cells.

HEK293 cells were grown in DMEM media (catalogue #30-2003, ATCC, Manassas, VA, USA) supplemented with 10% Fetal Bovine Serum, (Gibco/

Invitrogen catalogue #16000-044), 2% Penicillin/streptomycin (Invitrogen catalogue #15070-063, prepared with 5000units/ml penicillin, 5000 mg/ml streptomycin sulphate in 0.85% saline), and G418 antibiotic (Sigma cat. no. G8168) at varying concentrations. Cells were incubated at 37 °C in a humidified atmosphere of 5% CO_2 in a Napco CO_2 5400 Growth chamber. Falcon cell culture flasks (250 ml) were used for growth and maintenance, and 100mm dishes were used in plating cells for transfection. Cells were split into new flasks when 95-100% confluent (usually weekly). Following removal of culture medium, cells were washed once with 10 ml of warm Dulbecco's phosphate buffered saline (DPBS, placed in 37 °C water bath ~20 minutes before use), then incubated 60 seconds with 5 ml of warm trypsin (0.25% trypsin EDTA, Gibco/Invitrogen, Carlsbad, CA) and re-suspending in 10 ml new DMEM. Re-suspension was performed by repeated up and down pipetting using a transfer pipette. Typically, 0.5 ml of the cell suspension was diluted with 24.5 ml of warm growth media and the mixture transferred to a new flask. Cell culture flasks were re-used a maximum of three times, and handling of cells was performed under semi-sterile conditions: Bottles, gloves, and other equipment were wiped with 70% aqueous ethanol before being used under a laminar flow hood pre-exposed to UV light for one hour.

2.3.2 Dose response for HEK293 cells incubated with G418.

Prior to transfection, a kill curve (dose response curve) for HEK293 by antibiotic G418 was established (BD Biosciences protocol #PT3132-1, version #PR43789). Briefly, untransfected HEK293 cells were plated at a cell density of 10^6 cells/cm^2, and incubated in normal media and growth conditions (described above) with G418 added over a range of concentrations. The optimal concentration is considered to be that which results in 90% cell death in one week (ED_{90}) and 100% death within two weeks. Cells are considered dead when they become round and fail to adhere to the dish. Based on these criterions, it

was determined that the optimal G418 concentration in which to grow the cells was between 0.2 and 0.4 mg/ml.

2.3.3 Stable Transfection of HEK293 cells with AChBP plasmid.

Stable transfections were performed using the Qiagen SuperFect reagent kit and protocol (Qiagen, catalogue #301307). Cells were maintained in G418-free medium for 48 hours directly following transfections. A sample of the medium was taken at this point and assayed for AChBP expression using radiolabelled ^{3}H-epibatidine. Medium was then replaced with fresh DMEM containing either 0.4 mg/ml or 0.3 mg/ml G418. The 0.4 mg G418/ml line was transfected using the standard 30 μl: 5 μg superfect:DNA ratio suggested by the Qiagen protocol. Cells recovered very slowly and over one month of incubation was required before sufficient cells were obtained to permit efficient harvesting of the expressed AChBP. Cells grew well after this point. The 0.3 mg G418/ml line was transfected using an optimized 50 μl: 5 μg superfect:DNA ratio. This cell line showed faster growth and produced a usable cell line in about 2 weeks.

2.4   Growth and harvest of AChBP from transfected cell media.

The 0.4 mg/ml G418 cell line was chosen for expression of AChBP. Stably transfected cells were maintained in 250 ml, 75 cm^2 cell flasks until they reached 95% confluence. They were then transferred to larger dishes suitable for large scale protein production. Cells were washed once with PBS, incubated 60 seconds with 5 ml trypsin, and resuspended in 10 ml media by pipetting 10-20 times against the bottom of the flask. 2.5-3.0 ml of resuspended cells were transferred to large cell culture dishes (VWR catalogue #BD351040, 600 cm^2) containing 110-130 ml of 0.4 mg/ml G418-containing media (described above). Cells were incubated as described above, and cell culture media was collected every 2-4 days, usually at days 3, 5, and 7, corresponding to confluence levels of about 30%, 80% and 95%, respectively.

2.5   Purification of AChBP.

AChBP was purified from the cell culture medium using Sigma Nickel-EDTA His Select Columns. Collected medium was prepared for purification by addition of salts to concentrations of 50 mM Na_2HPO_4, 0.3 M NaCl and 10 mM imidazole. Sodium hydroxide (1 M, about 25 ml per 500 ml media) was used to adjust the pH to 7.5, and the media was filtered through 0.4 or 0.2 μm cellulose acetate filters. This protocol is a modification of the Sigma His-Select column product H8286 protocol. The addition of NaCl served to increase the ionic strength of the solution and imidazole is used to decrease non-specific binding to the affinity column. Adjusted culture medium was loaded onto equilibrated Nickel-EDTA His-Select columns (Sigma #H8286) at a flow rate of 1 ml/min using a peristaltic pump. The medium was placed on ice for the duration of this process, which lasted 2-5 hours. This process was preceded and followed by equilibrating the column with 5-10 ml/column of a media-free equilibration buffer, also 50 mM Na_2HPO_4, 0.3 M NaCl, 10 mM imidazole, and adjusted with sodium hydroxide to pH 7.5. Elution was accomplished with 5-7 ml/column of a PBS buffer made similarly to the equilibration buffer above, except sodium hydroxide is replaced with 250 mM imidazole. Elution was performed in 1.5 ml fractions, with most of the AChBP appearing in the second fraction.

AChBP was found to elute with significant amounts of imidazole, which required removal since it interfered with protein quantification. To remove imidazole, we first utilized membrane dialysis using a 12-14 kilodalton (kD) molecular weight-cutoff dialysis tubing overnight in 1000-fold excess of phosphate buffered saline (PBS, used for scintillation proximity assay (SPA) described below). While this method was effective, it was more efficient to use 30 kD MW-cutoff MicroSep centrifugal filters (Pall life Sciences, Ann Arbor, MI). Use of MicroSep filters produced equally pure AChBP in about 2 hours. Eluant was applied to filters then concentrated by centrifuging at 6000 g for 40 minutes.

Two washes of 3-4 ml PBS/wash were performed to remove excess imidazole and the protein was removed from the filter by addition of 1 ml of PBS.

2.6   Analysis of AChBP using Lowry Assay and Electrophoresis.

Expression and purification of AChBP from the 0.4 mg/ml G418 cell line yielded about 1-4 mg protein per litre of medium, as determined by Lowry assay, (Sigma's Micro Lowry Kit, Peterson's Modification, Catalogue #TP0300).

Gel electrophoresis was performed under non-denaturing (TG buffer, BioRad native sample buffer), and denaturing (TGS buffer, Laemli sample buffer) conditions, using standard BioRad procedures, on a BIO-RAD *Mini-Protean 3 Cell.* BioRad kaleidoscope standard was used, and constant 200 V was applied for 20-35 minutes until the dye front was close to the end of the gel. Precast 7.5% and 12% tris-HCl BioRad gels were used in all experiments. AChBP was identified as the 30 kD band under denatured conditions and about 150 kD under non-denaturing conditions. No bands of similar molecular weight were observed in a control untransfected-HEK293 media sample.   Since the non-denatured protein was approximately 5 times the size of the denatured protein it was concluded that the protein expressed as a pentamer as expected. No bands were observed corresponding to any other stoichiometry including dimers or trimers. The AChBP in samples was visually estimated to be up to approximately 90% pure.

Purity of the AChBP had no observed effect on later scintillation proximity (SPA) assay. Since the SPA beads use nickel affinity to binding the AChBP, preparation of the beads essentially constitutes a second purification step. In addition, since any contaminating proteins are unlikely to bind LGIC ligands, a very low non-specific binding was observed. Media purified from untransfected cells gave little or no SPA response (data not shown) even at high levels of radioligand. The "non-specific" binding observed with high levels of [3]H-

granisetron and epibatidine on AChBP-treated SPA beads is thus likely due to binding at secondary, low affinity sites on the AChBP protein itself.

2.7   Vacuum drying of AChBP.

In order to facilitate storage and increase stability of the AChBP, we attempted to dry the purified AChBP then reconstitute it. We determined that the AChBP was resistant to denaturation under these conditions and could be easily dried and reconstituted. Stability was greatly increased in dried samples. Prior to drying, the AChBP was concentrated to 700 μg/ml in PBS, aliquotted into 200 μL portions, and placed in 0.5 ml micro-centrifuge tubes, un-capped. Tubes were spun under vacuum in a rotatory evaporator (DNA Speed Vac model DNA 110, Savant Instruments, Holbrook NY: "drying rate" on low, "concentrator" on) at ambient temperature for two or three hours until dry. Dried samples were then refrigerated for up to 12 months at 2-8 °C. No differences in protein composition or binding characteristics were observed using PAGE or SPA assays between samples taken before drying, immediately after drying, or after several months of storage. This topic is covered in more detail in chapter three.

2.8   Scintillation Proximity Assay (SPA).

Scintillation Proximity Assay (SPA) provides a rapid, high-throughput assay for evaluation of receptor ligands. This assay differs from a conventional ligand binding assay in that the protein is bound to a suspended bead matrix coated with copper. AChBP was bound to the beads using the 6X His tag. Scintillant is integrated into the bead matrix. Only radioligand bound at close proximity to the bead excites the scintillant. Using this system, no filtration is necessary for the separation of bound and unbound ligand since only bound ligand produces a signal. This enables both rapid analysis of binding data and the use of low affinity ligands.

In our assays, PVT Copper His-tag SPA beads (GE/ Amersham #RPNQ0097) were diluted with phosphate-buffered saline to 0.1 or 0.5 mg beads per ml, and optimized amounts of His-tagged AChBP were added. Bovine Serum Albumin (BSA, Sigma; 2 mg/ml) was added to decrease non-specific binding. Mixtures were incubated at ~21°C (room temperature) for approximately one hour before ligands were added, and samples were counted a few hours to a day later on a 1450 Microbeta Plus liquid scintillation counter (Perkin-Elmer). Counts were taken over one minute at a time every five minutes for at least 25 minutes, and then averaged. Data reported results from the average and standard error of at least four experiments performed on different days.

2.8.1   SPA ^{3}H-epibatidine and ^{3}H-granisetron binding.

For ^{3}H-epibatidine radioligand binding, 0.1 mg/ ml beads in phosphate buffered saline (PBS, see appendix 2), were incubated one hour with 2 mg/ ml BSA, and 0.0125 nM AChBP. Three ml of this suspension was added to 4-ml scintillation vials. Seven concentrations of ^{3}H-epibatidine were added increasing by three-fold from 0.004 nM to 3.0 nM. These and one zero were capped and shaken for one minute, incubated for one hour at room temperature, and then counted. At B_{max}, a typical response was 1000 counts per minute (CPM), with a percent error of about 5%. ^{3}H-epibatidine radioligand was obtained from GE/ Amersham Biosciences and had an activity of 53.0 Ci/mmol.

^{3}H-granisetron binding was performed similarly, except 0.5 mg/ml beads were used, and only 200 µl of beads/radioligand mix were required. ^{3}H-granisetron concentrations were varied between about 1.0 nM and 240 nM. Nonspecific binding was determined in the presence of 1.0 M acetylcholine, and was subtracted. Incubation time was increased to at least two hours. ^{3}H-granisetron was obtained from Perkin Elmer.

2.8.2 SPA Competition assays.

^{3}H-epibatidine (1.0 nM) was used as the radioligand in competitive binding assays. An AChBP concentration of 0.025 nM in 3 ml of PBS/BSA/Beads was used for all competition assays. At least 6 concentrations of competitor, flanking the K_i in 3-fold intervals, were used to acquire final data. Care was taken so that bound radioligand remained ≤10% of total ligand, assuming five binding sites for AChBP and data were corrected for loss of free ligand. The competing ligand was added before the radioligand, and incubated after shaking for at least two hours. However, variations on the incubation time had little effect on IC_{50} values. (Supplementary material is available for this section)

2.8.3 SPA Data Analysis.

Data was analyzed using Graph Pad Prism 4.0 software. The K_d values for ^{3}H-Epibatidine (using 0.0125 nM AChBP) and ^{3}H-granisetron (using 2.6 nM AChBP) were calculated using the simple one-site binding model shown in equation 1:

Equation 1 $$Y = B_{max}^{*}X / K_d + X,$$

where X is radioligand concentration and Y is the response in CPM (proportional to bound ligand). For epibatidine, the non-specific binding signal (as determined independently by competition with excess competitor), was <<10%, and was ignored. Non-specific interaction of granisetron with AChBP-bound beads was linear with ligand concentration, and was determined in parallel experiments and subtracted. The IC_{50} for the inhibition of epibatidine, and Hill-slopes (n) were determined for ligands using the sigmoidal dose-response equation and Graph pad Prism software:

Equation 2 $$Y = Bmax / (1 + 10^{([log(IC50)-X] * n)})$$

where X is the logarithm of the concentration of cold ligand, Y is the response in CPM, and n is the Hill slope. The K_i was calculated using the Cheng-Prusoff equation: $K_i = IC50 * (K_{d(epi)}/[epi])$. Data for individual experiments were normalized by dividing by the experiment's calculated B_{max} so that experiments with different B_{max} values could be compared and/or combined.

2.9   Surface Plasmon Resonance (SPR).

Surface Plasmon Resonance (SPR) assays were carried out using a BiaCore 2000 plasmon resonance instrument (BIACORE AB, Uppsala, Sweden) and the BiaCore CM5 Sensor Chip and other appropriate chips. These chips were used to immobilize anti-Flag antibodies or the AChBP itself. AChBP purified from the Sigma His-Select columns or eluted from polyacrylamide gels was directly identified using the anti-FLAG chip, thus allowing identification of the AChBP protein.

SPR detection of ligands is limited to molecules of molecular weight greater than 180 Daltons. For larger molecular weight compounds such as d-tubocurarine (dTC), and α-bungarotoxin, both SPA and SPR assays were used and therefore serve to validate each other in evaluating the performance of the AChBP. Mutants of the AChBP are also undergoing such testing. Comparing K_d values obtained with SPA versus SPR for compounds such as physostigmine could also be used to determine if the binding site for that compound is the primary binding site or an allosteric site. The SPR assay is particularly useful for obtaining information on and off rates of interaction, as well as thermodynamic information for large compounds if needed. For AChBP-SPR applications, the AChBP is immobilized on a CM-5 surface using the EDC/NHS method (amine coupling). Data generated by SPR is analyzed using BIAevaluation software, version 3.0. Kinetic rate constants are globally determined by fitting the biosensor data using numerical integration and nonlinear least squares analysis. Several binding models are available and a mass-transfer rate constant can be included

in the models to account for diffusion of molecules of analyte from the solution to the biosensor interface according to Fick's law, where appropriate [34].

2.10. Microcantilever (MC) Evaluation.

Microcantilevers (MC) have potential as sensitive, cost-effective biosensors for medical diagnostics and environmental testing. Microcantilever experiments were performed in Dr. Hai-feng Ji's laboratory at Louisiana Tech University by Dr. Ji and his students. The AChBP was used as published (Gao et al, [35]) to evaluate an improved method of adsorption of a self-assembled monolayer (SAM) film to a commercially available silicon-chromium-gold microcantilever (Veeco Instruments). This improved method employed a trifluoroacetic acid wash protocol to improve AChBP immobilization and binding response. To assure the quality of the AChBP was not affected by shipping to Louisiana, the AChBP provided to Dr. Ji was vacuum-dried (see section 2.7) and equivalent samples evaluated in our laboratory using SPA and SPR assays. AChBP was bound to the microcantilever using a method similar to what we employed for SPR, and the bending response of the cantilever to applied acetylcholine (indicating a conformational change in the protein) was measured. The improved method was critical to the observation of a conformational change of AChBP on binding acetylcholine. This work is further addressed in Chapter 3.

Chapter 3: The AChBP as a Molecular Biosensor

As described in Chapter 1, the soluble nature of the AChBP protein, its ease of handling and the similarity of its binding site to LGIC receptors makes it an ideal lead molecule for developing a family of biosensor proteins. To evaluate the feasibility of this idea, we utilized the wild type cloned AChBP protein (chapter 2) as a biosensing molecule on three different biosensor surfaces: scintillation proximity assay (SPA), surface plasmon resonance (SPR) and microcantilevers (MC).

This chapter describes the development of an expression system for AChBP, its purification, characterization and attachment to sensor platforms. The experiments in this section are designed to test Hypothesis 1 in section 1.10 (Chapter 1) of this thesis and address Objectives 1.1-1.4. These data demonstrate the effective production of the AChBP protein using HEK293 cells, and its successful utilization as a biosensor. The SPA experiments demonstrate its potential for high-throughput screening and the SPR and microcantilever experiments demonstrate its usefulness on chip-based instrumentation. In addition, its use in "conformational change-" based sensing demonstrates an improved technology for microcantilever biosensors. [35]

3.1   Introduction.

The acetylcholine-binding protein (AChBP) has been used extensively as a template for computer based modelling of the N-terminal domain of Cys-loop ligand-gated ion channels (LGIC's) [22, 23, 28-33]. In this chapter, its use as a biological sensor for detection of LGIC ligands is explored. As mentioned in chapter 1, the AChBP is known to bind ligands which also bind to nicotinic acetylcholine receptors (nAChR). While its broader specificity is unknown, structural similarities to other LGIC receptors suggest AChBP analogs could be

engineered to match the selectivity of other receptors including the GABA, Glycine and Serotonin type 3 receptors.

To be used as effective biosensor molecules, the AChBP proteins must be easily produced, purified and stored. In addition, the proteins must have a reasonably long shelf life (stability) and be able to be transported easily. Of course, they must also function correctly and provide a reasonable signal to noise ratio when attached to biosensor surfaces and exposed to ligands. This study aims to evaluate our cloned wild type AChBP protein from this perspective.

If the AChBP can be shown to meet the requirements for a biosensor molecule outlined above, it could be useful in a number of biosensor applications. Systems amenable to the use of AChBP type proteins include Scintillation Proximity Assay (SPA), as well as chip-based instruments such as Surface Plasmon Resonance (SPR), and Microcantilevers (MC). These systems differ in their potential applications, sensitivity, detection methods and cost.

3.1.1 Scintillation Proximity assay.

Scintillation proximity assay (SPA) is a bead-based assay that utilizes an affinity medium (SPA beads) coated with a scintillant. The receptor protein of interest is typically bound to the bead surface using either copper chelation or antibody binding. The protein/bead is then exposed to a radioligand and, after an appropriate incubation time, is placed in a scintillation counter to determine the amount of ligand bound in close proximity to the bead surface (figure 3.1). SPA represents a technological advance over conventional radioligand binding assays which have become the standard for obtaining LGIC pharmacological data (for examples, see [23, 33]). Conventional LGIC binding assays are often conducted similar to the SPA assay but all require filtration of the protein to separate bound and unbound ligand prior to scintillation counting. The incorporation of scintillant into the bead eliminates the filtration step since only radioligand bound in close proximity to the bead surface is capable of exciting the scintillant. Elimination of

the filtration step makes it easier to automate the technique and thus permits high throughput assays to be developed. Although SPA beads can also be used with ordinary cell-membrane homogenates, the SPA process is particularly well suited to a soluble protein such as the AChBP or engineered AChBP analogs.
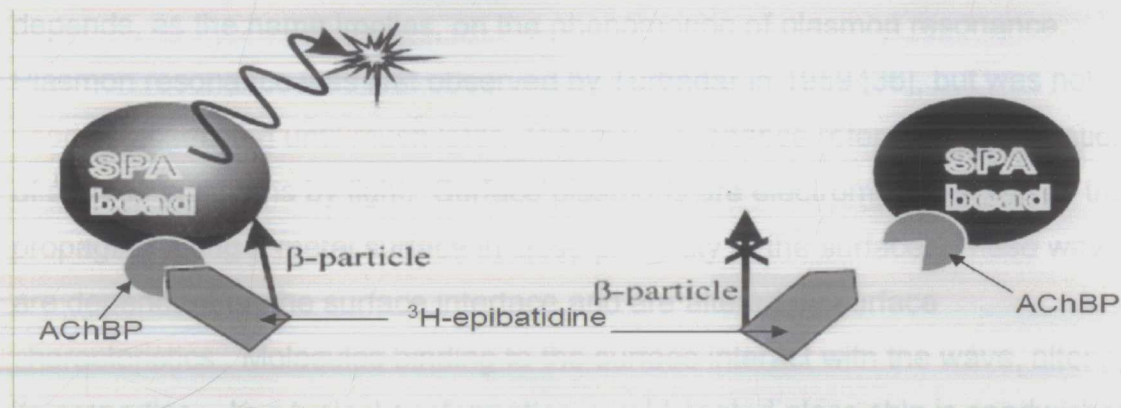
Figure 3.1. SPA Schematic. In the diagram at left, the radioligand is in close proximity to the bead, and the emitted β-particle causes the scintillant coating of the bead to emit a photon, which is detected by the counter. At right, unbound ligand is not close to the bead, and thus does not excite the scintillant. Diagram is not to scale: beads are 2-8 μm in diameter, the average path length for tritium (^{3}H) decay is 1.5 μm, AChBP pentamer 8 nm across, and ^{3}H-epibatidine radioligand is ~1nm long. Picture adapted from SPA Handbook (GE/ Amersham Biosciences).

The SPA process is quite simple: First, the receptor protein (such as the AChBP) is mixed with the SPA beads and an appropriate buffer. Copper on the SPA bead binds to the 6X His tag on the C-terminal of the AChBP, immobilizing the protein on the bead surface. Varying concentrations of ligand are added and the fraction of ligand bound to the protein/beads is determined by scintillation counting. An equilibrium binding constant (K_d) for the radioligand is calculated from a plot of radioligand concentration vs. fraction bound similar to conventional binding assays. Inhibition assays can also be used to determine the affinities (K_i values) of compounds not available in radiolabelled form. One major advantage over conventional assays which require a filtration step is the ability of using SPA assays with lower affinity ligands. Since filtration is not required, there is no danger of washing away a low affinity ligand during washing of the filters.

3.1.2 Surface plasmon resonance.

Surface plasmon resonance biosensing is a relatively new technology developed by Biacore Inc. (www.biacore.com). This chip-based technology depends, as the name implies, on the phenomenon of plasmon resonance. Plasmon resonance was first observed by Turbadar in 1959 [36], but was not used in biosensing until much later. Plasmon resonance refers to the excitation of surface plasmons by light. Surface plasmons are electromagnetic waves that propagate along a metal surface in close proximity to the surface. These waves are dependant on the surface interface and are altered by surface characteristics. Molecules binding to the surface interact with the wave, altering its properties. In a typical conformation a gold coated glass chip is sandwiched between a microfluidics cell and a prism (figure 3.2) Incident light is directed through the prism at an angle that produces total internal reflection. The incident light interacts with surface plasmons generated at the gold surface (and is influenced by the surface characteristics). This interaction alters the angle of reflection of the incident light and this change is monitored by the SPR instrument. Thus, the output of the SPR instrument is essentially a measurement of changes in this angle that correspond to ligand binding to the gold surface. These changes are directly related to the molecular weight changes at the gold/ buffer interface. Hence, SPR measures changes in molecular weight over time.

The gold surface of the plasmon resonance chip is typically coated with coupling reagents that allow proteins or small molecules to be attached to the chip surface. Since this technique measure changes in molecular weight, it works best when the lower molecular weight binding partner can be attached to the chip and the higher molecular weight molecule is placed in the flow cell. The detection limit for ligands binding to the chip for the Biacore instrument is typically considered to be about 180 atomic mass units (amu).
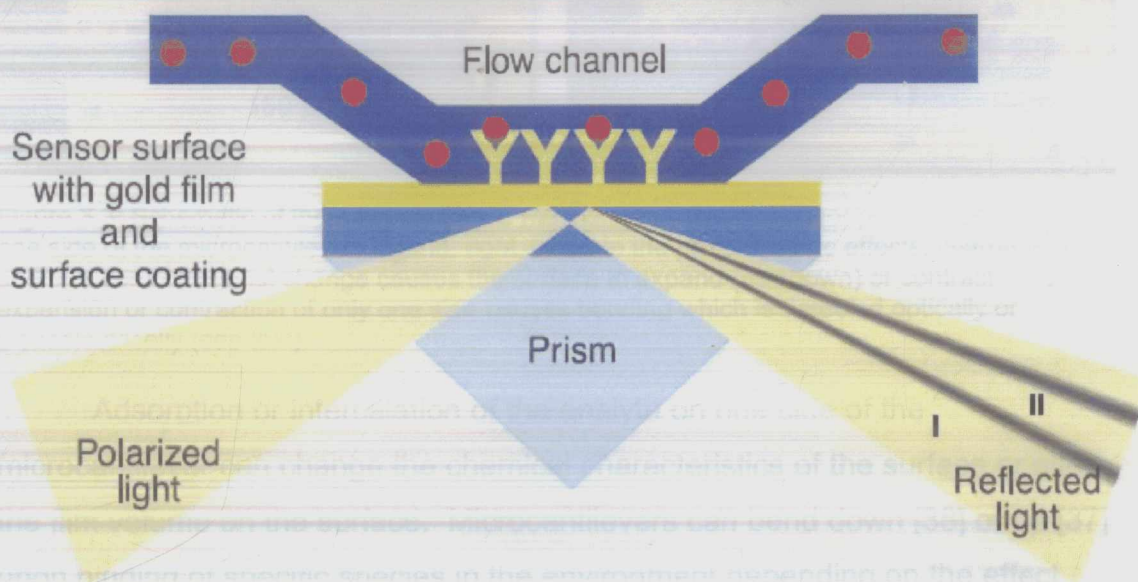
Figure 3.2. Schematic of the Biacore SPR system. The properties of the gold surface (yellow) change as molecules bind to the chip surface. These properties depend on mass of the molecule and the properties of the solution. Alterations of the gold/ solution interface alter the surface plasmon waves resulting in change in the angle of reflection. The Biacore 2000 instrument monitors this angle and produces and output measured in resonance units (RU). Picture from Biacore TN1 handbook[34].

3.1.3 Microcantilevers.

A microcantilever sensor is a metallic device that bends when molecules bind to one side. This bending can be detected using optical or piezoelectric methods (Figure 3.3) [37]. Microcantilevers have several advantages over conventional sensors including small size, great sensitivity and the ability to detect molecules that are not labelled. Microcantilevers are cost-effective and highly sensitive sensor platforms with potential applications in medical diagnostics, environmental monitoring, and high throughput analysis [38-40].
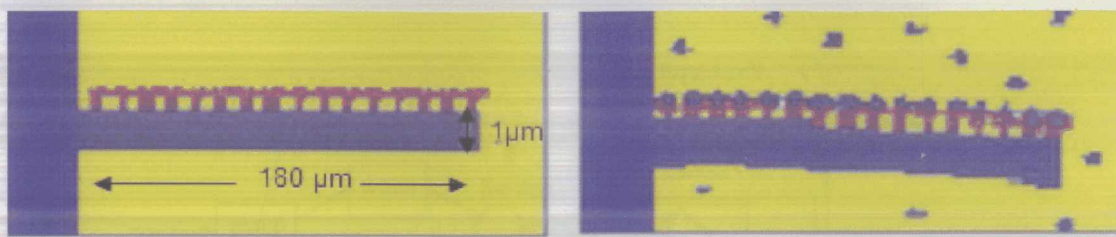
Figure 3.3: Schematic of the microcantilever mechanism. The biosensor protein (left) is bound to one side of the microcantilever. Ligand, right, binds to the protein; steric effects, charge effects and/or a conformational change causes the surface to expand (as shown) or contract. This expansion or contraction of only one side causes bending which is detected optically or piezoelectrically (see text).

Adsorption or intercalation of the analyte on one side of the microcantilever can change the chemical characteristics of the surface or alter the film volume on the surface. Microcantilevers can bend down [38] or up [37] upon binding of specific species in the environment depending on the effect binding produces. From a molecular point of view, the bending results from intermolecular interactions such as electrostatic attraction [37], repulsion [41], steric effects [38], or a combination of these, which alter the surface stresses on the cantilever. By monitoring changes in bending response of a cantilever, surface stress changes induced by adsorption or molecular recognition can be precisely and accurately recorded. Bending is easily detected optically using a system such as that shown in Figure 3.4. For piezoelectric detection, the microcantilever is mounted on a piezoelectric device and changes in the electrical properties of the piezoelectric stack that result from bending are measured. The advantages of piezoelectric detection are more sensitivity, increased stability and the ability to put a large number of microcantilevers directly into a microchip device.
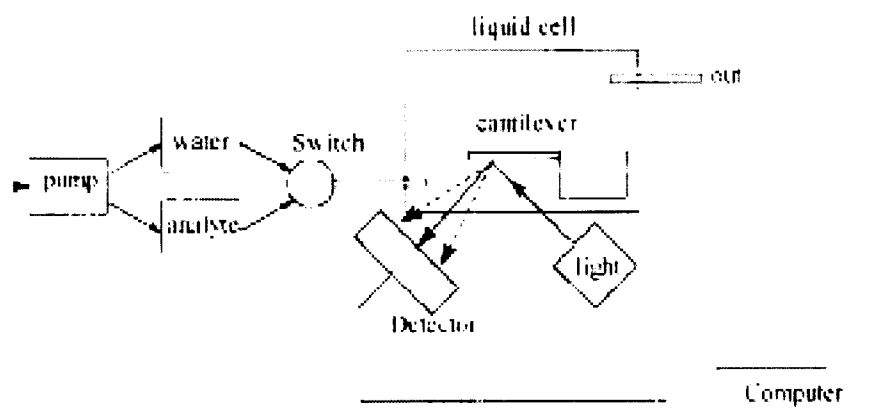
Figure 3.4. MC Schematic with optical detection. Analyte is introduced into the flow cell (liquid cell) via a switch. The bending of the microcantilever (MC) is detected as a change in position of the reflected light hitting the detector. Figure is reproduced from Gao et al. [35].

The microcantilever assays described in this thesis were done in Dr. Hai-feng Ji's laboratory. This work represents the first use of AChBP as a microcantilever biosensor and demonstrates an improved method of microcantilever coating, as described in section 3.2.6.

3.2 Materials and Methods.

3.2.1 Engineering of the AChBP biosensor protein.

AChBP DNA from *Lymnaea stagnalis* was synthesized commercially and inserted into the p3xFLAG-CMV-9 vector with a C-terminal 6x "His tag" and an N-terminal p3-Flag tag. The p3xFLAG-CMV-9 vector contains a gene that confers resistant to the antibiotic G418 for use in selecting transfected mammalian cells. This DNA was used to stably transfect HEK293 cells, which actively secrete AChBP into the surrounding media as described in chapter 2. The 6X C-terminal His tag allowed the protein to bind to metals such as copper and nickel, and was included as a rapid means of purifying the protein (using Nickel-EDTA columns, Sigma). The Flag tag was originally included to provide a secondary option for purification (using an anti-Flag affinity column) but was not used since the Nickel

affinity columns provided sufficient purity. The Flag tag was used in some of the SPR experiments as a way of identifying and immobilizing AChBP on the sensor surface, however; the preferred choice for SPR immobilization was amine linking as described below (section 3.2.5). An N-terminal flag, C-terminal 6x-His AChBP similar to this one was previously expressed by Hansen et al [42]. The His-tag and Flag tag were both shown to be accessible to purification (i.e. they were not buried) and the tags do not seem interfere with normal binding [3].

3.2.2 Expression/purification of AChBP.

AChBP was expressed and purified as described in Chapter 2. Briefly, His-tagged AChBP was expressed in HEK293 cells, which actively secreted the AChBP into the medium. AChBP-secreting cells took about 2-3 days to produce approximately 1 mg protein per litre of culture medium. While this is relatively modest yield, it should be noted that this is a large amount of protein for use in assays such as SPA and SPR. Medium was collected, buffered (pH 7, high ionic strength) and processed as described in section 2.5. The AChBP was extracted from this media using nickel-EDTA purification columns, and eluted with 250 mM imidazole. The protein was then pooled and concentrated in PBS to a concentration of 700 μg/ml using 30 kD MW-cutoff MicroSep centrifugal filters (see section 2.5). The AChBP was then dried and reconstituted prior to use. AChBP shipped for microcantilever analysis in Dr. Ji's laboratory was dried prior to shipping and reconstituted in Dr. Ji's laboratory with distilled H_2O.

3.2.3 Drying of AChBP.

We initially attempted to preserve AChBP by freezing AChBP-containing medium. This process significantly interfered with purification. Freezing the medium produced a precipitate that decreased the yield of AChBP to undetectable levels. As an alternative storage and transport method, we attempted to dry the protein.

AChBP was dried at room temperature under a vacuum. AChBP was concentrated to 700 µg/ml (5200 nM) in PBS, aliquotted into 200 µL portions, and placed in 0.5 ml micro-centrifuge tubes, un-capped. Tubes were spun under vacuum in a rotary evaporator (DNA Speed Vac model DNA 110, Savant Instruments, Holbrook NY: "drying rate" on low, "concentrator" on), spinning under partial vacuum at ambient temperature for two or three hours until dry. Samples were then refrigerated for up to 12 months at 2-8 °C. The reconstituted protein showed properties (binding and structural) identical to that of the freshly purified proteins (see section 3.3.1).

3.2.4 Scintillation Proximity Assay.

The SPA assay is performed similar to conventional radioligand binding assays as described in Chapter 2. Scintillation vials were read using a Perkin-Elmer Microbeta Plus Scintillation Counter. For SPA assays, SPA beads were mixed in a scintillation vial with medium containing the protein of interest (in this case AChBP). The AChBP binds to the copper chelated on the bead surface via the 6X His tag. Radioligand at the appropriate concentration was added, and (if desired) a competing ligand. The mixture was allowed to equilibrate (1-2 hours) before counting. Since only radioligand bound to protein on the bead surface can excite the scintillant, no separation of bound and unbound ligand by filtration is necessary. One of SPA's advantages as a bioassay is that it is at once both a purification step and an analysis.

As described above, imidazole was typically removed from the eluant during purification since it interferes with the Lowry assay used to determine the total protein concentration. However, removal of the imidazole was not necessary in order to observe high-affinity binding of ^{3}H-epibatidine using SPA assay. We observed that imidazole appears to improve the stability of AChBP in solution when stored at 2-8 °C (data not shown), probably due to stabilization of the single pentamer structure and preventing "clumping" of individual proteins.

Hansen et al [25] observed pentamer-dimerization of AChBP on storage. In addition, we discovered that the AChBP is not stable for long periods when diluted to ~15 nM in the PBS used for the SPA assays. Hence for SPA assays, the AChBP was diluted with PBS immediately before addition of the SPA beads.

3.2.4.1 Binding of ^{3}H-epibatidine.

For evaluation of ^{3}H-epibatidine binding, the protein was diluted to 15-50 nM in PBS, then further diluted with an SPA bead suspension (0.1 mg beads/ml beads and 2 mg BSA/ml in PBS (see appendix 2)) to a final concentration of 0.0125 nM AChBP. After a one hour incubation period, three ml of this suspension were added to 4-ml scintillation vials. Seven concentrations of ^{3}H-epibatidine were added increasing by three-fold from 0.004 nM to 3.0 nM (final concentrations). The ^{3}H-epibatidine samples and a control sample (no ^{3}H-epibatidine) were capped and shaken for one minute then incubated for one hour at room temperature prior to counting using a scintillation counter. At saturating concentrations of ^{3}H-epibatidine, the calculated B_{max} was typically about 1000 counts per minute (CPM). Nonspecific binding was considered to be the binding observed in the presence of a saturating concentration of a second, competitive ligand. In these experiments, nonspecific binding was comparable in magnitude to the instrumental background noise (10-50 cpm); thus it was ignored in the ^{3}H-epibatidine K_d calculations. The high sensitivity for specific binding and low non-specific binding was found to be an advantage of the SPA assay system.

3.2.4.2 Binding of ^{3}H-granisetron.

^{3}H-granisetron binding was performed similarly to ^{3}H-epibatidine binding described above, except that the bead suspension contained 0.5 mg beads per ml, 2.6 nM AChBP final concentration, and only 200 µl of bead suspension per sample were required. ^{3}H-granisetron concentrations were varied between 1.0 nM and 240 nM. Nonspecific binding was determined in the presence of 1.0 M

acetylcholine, and was subtracted from total binding to give specific binding. Nonspecific binding was about 5% or less of total binding. This increase in non-specific binding compared to that obtained using ^{3}H-epibatidine is likely due to the lower affinity of ^{3}H-granisetron and thus the use of much higher concentrations than were employed in the ^{3}H-epibatidine experiments. Incubation time for granisetron was at least two hours.

3.2.4.3 SPA Competition assays.

^{3}H-epibatidine (1.0 nM) was used as the radioligand in competitive binding assays. Competition experiments used 3 ml of 0.025 nM AChBP in bead/ PBS suspension. At least 6 concentrations of competitor, flanking the K_i in 3-fold intervals, were used to acquire final data. Care was taken so that bound radioligand remained ≤10% of total ligand and free ligand concentration was calculated as Total ligand – Bound ligand. The competing ligand was typically added before the radioligand, and the combined mixture was incubated after shaking for at least two hours. Variations on the incubation time had little effect on IC_{50} values.

3.2.4.4 SPA data analysis.

Data was analyzed using Graph Pad Prism 4.0 software. The K_d's for ^{3}H-epibatidine (0.0125 nM AChBP) and ^{3}H-granisetron (2.6 nM AChBP) were calculated using the simple one-site binding model:

(Equation 3.1) $$Y/B_{max} = X / K_d + X$$

where X is radioligand concentration and Y is the count per minute response (proportional to bound ligand). For epibatidine, the non-specific binding signal (radioligand interacting directly with beads or non-specifically with AChBP), was <10%, even at twenty times the K_d, and was ignored. Non-specific interaction of granisetron was linear with ligand concentration, and was determined in parallel experiments and subtracted. The K_i (from IC_{50}) for the inhibition of epibatidine,

and Hill-slopes were determined for ligands using the sigmoidal dose-response equation and Graph pad Prism software:

(Equation 3.2) $\quad$ $Y/B_{max} = 1 / (1 + 10^{([log(IC50)-X]~*~Hill~slope)})$

where X is the logarithm of the concentration of cold ligand and Y is the response in CPM. The K_i was calculated using the Cheng-Prusoff equation: $K_i = IC_{50}~*~(K_{d(epi)}/[epi])$.

3.2.5 Surface Plasmon Resonance (SPR).

Plasmon resonance assays were performed using the BiaCore 2000 plasmon resonance instrument and Biacore CM5 Sensor Chips. CM5 sensor chips are designed for use in immobilizing proteins using EDC/NHS amine linking [43]. We typically linked the AChBP directly to the chip surface although we also used chips cross-linked with anti-Flag antibody to capture AChBP. The carboxymethyl dextran surface of a Biacore CM-5 chip was first activated by injecting a 1:1 ratio of 0.4 M EDC and 0.1 M NHS for 14 minutes at a flow rate of 10 μL/min. Purified AChBP was diluted to 68 μg/mL in 10 mM sodium acetate, pH 4.0, and was injected for 10 minutes to achieve an optimum density. This method was optimized by varying pH and injection time using standard Biacore methods. The remaining activated surface groups were blocked with 1 M ethanolamine, pH 8.0. AChBP density was approximately 8000 resonance units (RU). Anti-Flag affinity chips were made using a similar procedure.

AChBP purified from the Sigma His-Select columns or eluted from polyacrylamide gels was directly identified using the anti-FLAG chip, verifying the accessibility of the Flag tag on the AChBP protein.

3.2.5.1 Binding of ligands to SPR-AChBP biosensor.

AChBP was immobilized on one or more of the four available flow cells on the Biacore CM5 chip. Another flow cell (typically flow cell 1) served as a control cell. To prepare the control cell, the surface was activated with EDC/ NHS and then blocked with ethanolamine. All SPR data were determine by subtraction of the sample cell (containing AChBP) – the control cell (ethanolamine blocked surface). This eliminates effects due to buffer effects on refractive index and non-specific binding to the chip surface. A series of nicotinic acetylcholine ligands were evaluated to test the functionality and sensitivity of the AChBP prepared SPR chip (dTC, physostigmine, galanthamine). A concentration series of each compound was injected to allow for determination of accurate kinetics. Duplicate samples of ligand were injected for 120 seconds at a flow rate of 50-75 μL/min. Dissociation of ligand from immobilized AChBP was monitored for 2-5 minutes. After dissociation, 10 mM Glycine, pH 2.5 was injected for 60 seconds at a flow rate of 50 μL/min to regenerate the surface. After regeneration, a stabilization time of 60 seconds was allowed between samples. Mass transport tests were also included in the analysis of all the compounds.

3.2.5.2 SPR biosensor data analysis.

Responses observed on a reference surface were subtracted from the binding responses obtained from the reaction surfaces. The average responses from buffer injections (0-concentrations) were also subtracted to remove systematic effects. Data were analyzed using BIAevaluation software, version 3.0. Kinetic rate constants were determined by global curve fitting using standard Biacore 1:1 binding models and non-linear regression techniques (BIACORE AB, Uppsala, Sweden).

3.2.6. Preparation of Microcantilever sensors.

Microcantilever experiments were developed and executed by Dr. Ji's laboratory at the Institute for Micromanufacturing, Louisiana Tech University, Ruston, Louisiana (Gao et al. [35]). These experiments used commercially available silicon microcantilevers (Veeco Instruments). The dimensions of the V-shaped silicon microcantilevers were 180 μm in length, 25 μm in leg width, and 1 μm in thickness. One side of these cantilevers was covered with a thin film of chromium (3 nm) and followed by a 20-nm layer of gold, both deposited by electron-beam evaporation. The uncoated side of the commercial microcantilever was silicon with a 12-19-Å-thick, naturally grown SiO_2 (native oxide) layer. All the chemicals were used as received from Sigma-Aldrich. Proteins were immobilized on the gold side of the microcantilevers.

The most commonly used functional groups for attachment of bioreceptors are carboxyl and amino moieties [35], which are usually introduced on the microcantilever by exposure of the gold surface to the corresponding amino or carboxyl groups containing thiol compounds. The thiols form a monolayer on the gold surface through a well-known self-assembly process. After monolayer formation, the bioreceptors are conjugated on the surfaces through crosslinking reagents. One of the most widely used cross-linking procedures uses 1-ethyl-3-(3-dimethylaminopropyl)carbodimide hydrochloride (EDC) and N-hydroxy-succinimide (NHS) to activate the surface (Figure 3.5). While widely used for multiple sensor devices, it has often been observed [44] that microcantilevers modified by a typical EDC/NHS process either did not deflect ligand when exposed to analyte or did not generate reproducible results. This poor performance of the microcantilever has been postulated to be due to either low packing density or defective surface coatings.
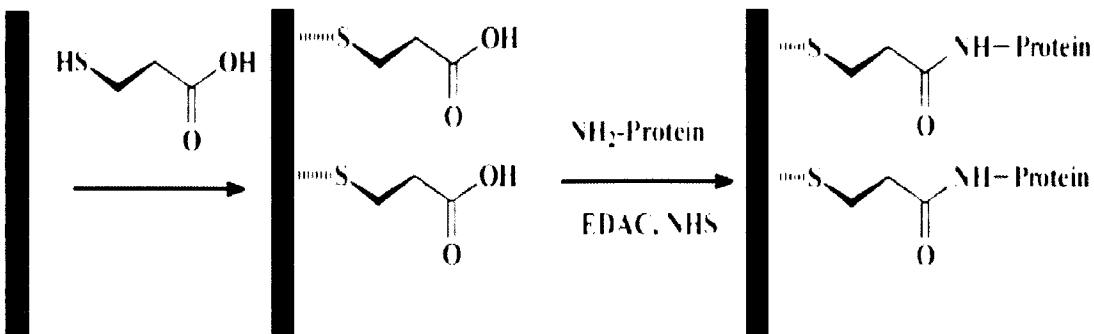
Figure 3.5: Surface conjugation chemistry of proteins on gold surface using the EDC/NHS pair. From Gao et al [35].

Recently, Wang et al [45] investigated the surface characteristics of the amino and carboxyl topped monolayers generated from thiol compounds and observed unwanted particles on the surfaces. They further suggested the coexistence of trifluoroacetic acid (CF_3COOH) with the thiols during SAM process for a smoother and cleaner surface. From these observations, it is reasonable to hypothesize that the unwanted particles inhibit the EDC/NHS crosslinking process. Removal of the particles on the surface prior to activation should improve microcantilever performance. Dr. Ji's laboratory utilized an improved cleaner protocol (see section 3.2.6.1) to improve the performance of their microcantilever system.

3.2.6.1. A new method of microcantilever surface modification.

Dr. Ji's laboratory [35] reported the effect of a clean monolayer surface (in which CF_3COOH has been incorporated) on microcantilever sensing performance, focusing on protein-based sensors. Two methods of microcantilever preparation are discussed. The first, 'Method A,' is the standard method, which is found to be inferior to 'Method B,' the new method utilizing CF_3COOH.

A typical EDC/NHS surface procedure (Method A) for protein immobilization is the following: The microcantilevers were thoroughly cleaned

with piranha solution and rinsed with water. The microcantilevers were then immersed for a 15-hour period in a 1 mM solution of 11-mercaptoundecanoic acid (MUA) in ethyl alcohol (EtOH), followed by rinsing in ethyl alcohol. Next, the microcantilevers were immersed in a 0.05 M 4-morpholine-propanesulfonic acid (MES) buffer solution containing 100 mg/ml of EDC and 100 mg/ml of NHS (pH = 6.8) for 30 minutes at room temperature, and then immersed in a 2 mg/mL proteins in MES solution for 3 hrs, followed by rinsing in the MES buffer solution.

In the modified approach (Method B), the first monolayer formation process was modified by adding 0.2 mL of CF_3COOH in the 1 mM solution of MUA in ethyl alcohol solution mentioned above. After 15 hours immersion in this solution, the microcantilevers were washed with EtOH, 10% (v/v) NH_3-H_2O/EtOH, and then EtOH. The remainder of the procedure was the same as described above for Method A.

3.3   Biosensor results and discussion.

3.3.1   AChBP expression and characterization.

Quantification of protein concentration by Lowry assay (data not shown) indicated expression levels of approximately 1-4 milligrams AChBP per litre of culture medium collected from the 600 cm^2 culture dishes. Non-denatured polyacrylamide gel electrophoresis (PAGE), (Figure 3.6) showed a distinct band of protein equivalent to a molecular weight of about 150 kD. SDS-PAGE conducted under denaturing conditions yielded a clear band of protein equivalent to about 30 kD. These molecular weights are consistent with literature values for AChBP and indicate the secreted protein assembles correctly with a pentameric structure.
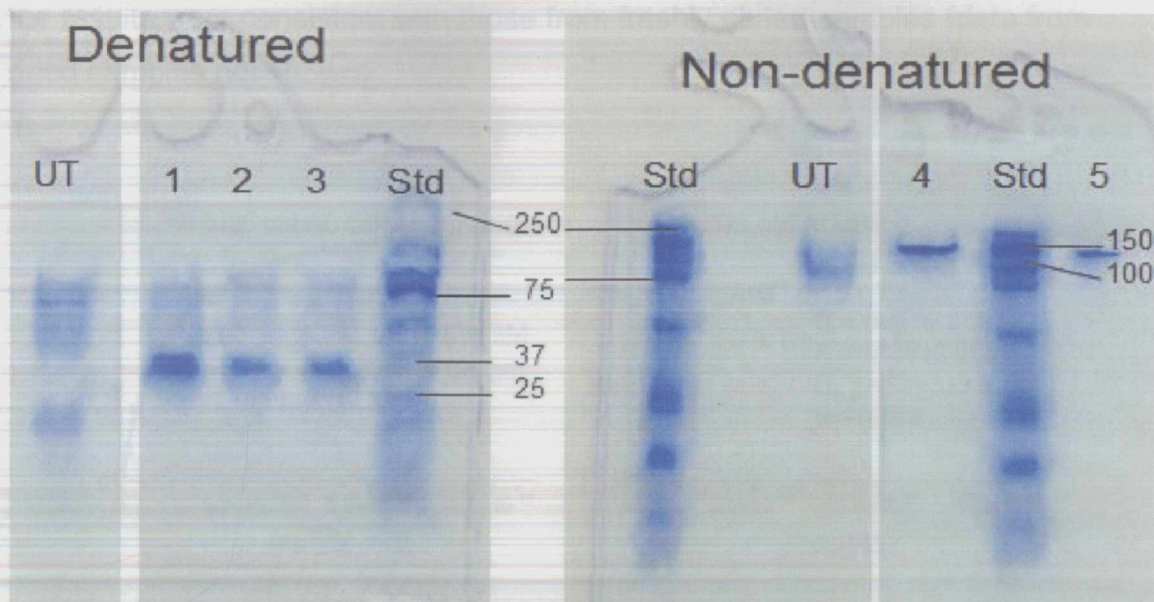
Figure 3.6. Acrylamide gel of AChBP. *Denatured:* A single, 7.5% polyacrylamide gel, Denatured (SDS): UT is a typical fraction from untransfected cells. Lanes 1-3 are typical of AChBP-transfected cells; the AChBP protein migrates to a region between 25 and 37 kD; lane "Std" contains BioRad Kaleidoscope standards; sizes in kilodaltons (kD) are indicated. *Non-denatured:* A second, 12% polyacrylamide gel, Non-denatured (no SDS): Lanes labelled "Std" are BioRad Kaleidoscope standards; sizes in kilodaltons (kD) are indicated. UT is from untransfected cells; Lanes "4" and "5" are from AChBP-transfected cells. The AChBP protein migrates to a region equivalent to almost 150 kD. Gels were stained with coomassie blue stain (BioRad). Some lanes were removed to save space.

3.3.1.1 Characterization of dried/reconstituted AChBP.

AChBP was dried as described in section 3.2.3 above. Reconstituted protein and freshly prepared protein (in solution) were compared to determine if the vacuum drying process had any observable effect on protein function. Reconstituted protein yielded similar Lowry results (100% recovery of total protein) and produced identical binding data using the SPA assay when compared to proteins that had not been dried (figure 3.7). We evaluated reconstituted protein immediately after drying and after several months of storage. Sodium dodecyl sulphate (SDS) and native (non-denatured) polyacrylamide gel electrophoresis (PAGE) were performed on the products, and

the results were consistent with those from freshly eluted samples (data from dried samples not shown).
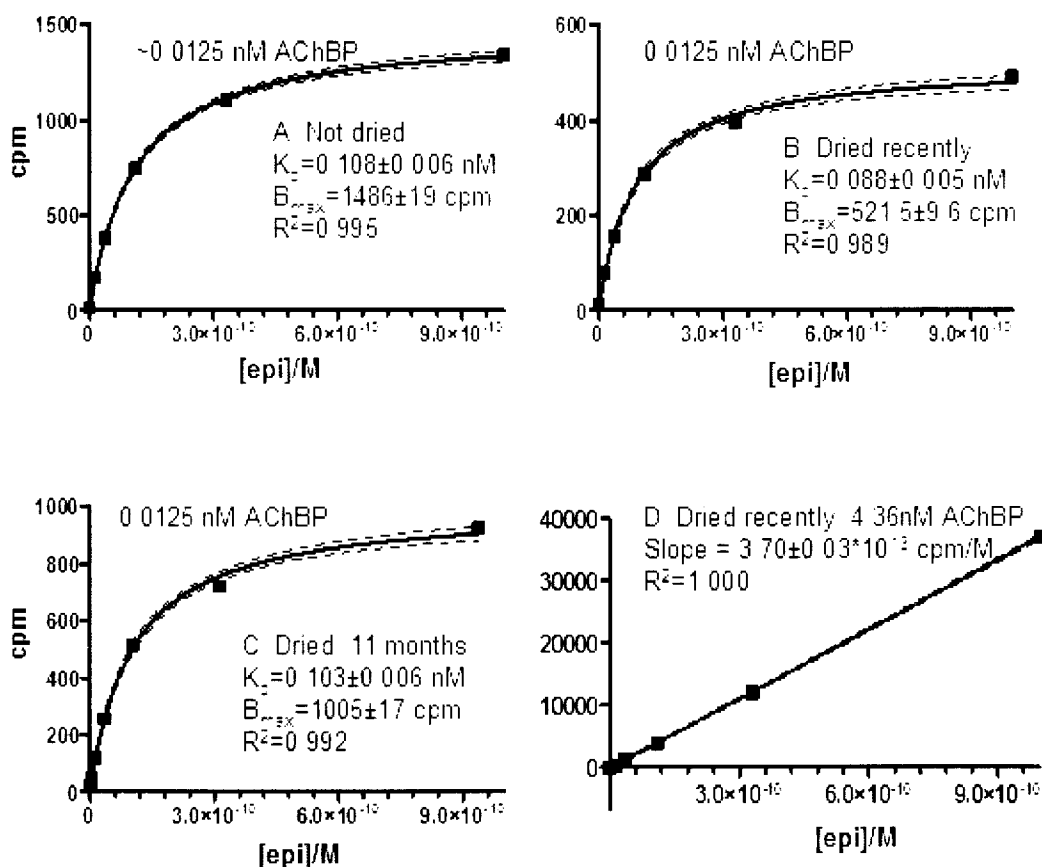
Figure 3.7. Effects of drying on AChBP binding kinetics. Concentrations of AChBP and ^{3}H-(+)Epibatidine (epi), observed K_d and B_{max} for each experiment, plus or minus standard deviation SD (except in graph D, where the 95% CI is given instead of SD, and R^2 for each graph are indicated. Dotted lines indicate 95% confidence intervals (CI). The nonspecific binding signal was 40±10 cpm at 1.0 nM, and was ignored in A-C. A. AChBP was eluted in 0.1% ascorbic acid and stored for about 3 weeks before removal of imidazole and use for SPA. This is the freshest AChBP for which we have good K_d data; However, this age should not be considered problematic, based on Hansen et al [42]. B. After drying AChBP by the method described above. This AChBP was from the pooled sample that was to be used for microcantilever work. The Bmax is probably low (compared to C) because the AChBP was not allowed to dissolve fully before dilution. The observed lower K_d is probably a related artefact (note, however, that this K_d difference is not statistically significant). C. represents the pooled AChBP after storage of one year. Note similarity of K_d and B_{max} to graph A. D. Counting efficiency of this method is about 10%, based on given epi activity of 53.0 Ci/mmol.

3.3.2 Binding Affinity of nAChR ligands to the AChBP by SPA.

Scintillation Proximity Assay (SPA) proved to be a fast, effective way of determining binding properties of various ligands to the AChBP. Pharmacological data compares well with data for previously expressed AChBP's [3], [42].

Table 3.1 shows the binding of a series of nicotinic acetylcholine receptor ligands with the AChBP prepared by the methods described above. Data were obtained using the SPA assay. The table includes results obtained in our assay in comparison to those obtained previously by Smit et.al. and Hansen et al. Smit and Hansen expressed AChBP in two different expression system (yeast and HEK293 cells).

Table 3.1. Our AChBP SPA results compared with literature. Data shown are Ki values extracted from the indicated published reports (columns 2-3) or determined in this study (column 4) using ^{3}H-epibatidine as the radioligand.

Compound	Smit et. al. (2001) [3] (Yeast)	Hansen et al. (2002; 2004) [25, 42] (HEK293)	K_i values for inhibition of ^{3}H-epi binding
α-bungarotoxin	2.6 ± 0.6nM	1.8 nM	3.6 nM
d-tubocurarine	93 ± 3 nM	150 nM	13.6 nM
Nicotine	98 ± 25 nM	86 nM	47 ± 5 nM
Epibatidine	1.4 ± 0.1 nM	0.16 nM	0.12 ± .01 nM
Acetylcholine	4.2 ± 1.1 µM	0.89 µM	1.6 ± 0.1 µM
Serotonin	269 ± 67 µM	Not available	91 ± 15 µM

Little difference was observed between expression system except for acetylcholine and epibatidine. Smit observed a 4.7- fold lower affinity binding for acetylcholine and an 8.8- fold lower affinity for epibatidine using the yeast expression system when compared to the HEK293 system. Our data was obtained using expression in mammalian HEK293 cells and is comparable to Hansen et al. The most substantial difference in affinity between our data and Hansen's was with d-tubocurarine. We observed an 11- fold higher affinity for dTC in our system. Differences in binding affinities are likely due to small differences in the experimental conditions although the specific affect of the

expression system on nicotinic agonists suggests that differences in post-translational modification may be slightly altering receptor mechanism. While the AChBP is not a ligand gated ion channel, it has been shown that conformational changes on binding of agonists do occur and that the protein likely shifts from a low affinity to high affinity agonist binding conformation. The similarity of our data to that obtained by Hansen et al validates the SPA as a sensor platform and demonstrates the successful production, synthesis, storage and attachment of the AChBP. The SPA technique is significant since it provides a rapid, low cost and easily accessible sensor platform for high throughput analysis. This approach is utilized to evaluate serotonergic ligand binding on the AChBP in chapter 4 of this thesis.

3.3.3 Binding of nAChR ligands evaluated by SPR.

To evaluate of the performance of the AChBP in Surface Plasmon Resonance (SPR) assays, purified AChBP was immobilized on CM-5 SPR chips using the EDC/NHS approach. Crosslinking of the AChBP yielded immobilization levels of approximately 3000 RU; sufficient for analysis of ligands over 200 amu. Figure 3.8 shows a series of sensorgrams obtained in a typical SPR experiment to determine binding kinetics of dTC to a CM-5/AChBP surface. dTC produced a maximum response of 100 RU. Typically, a response of 10-20 RU is sufficient for accurate determination of rate constants. At lower concentrations of dTC (<100 nM) the rate of binding was sufficiently slow to determine association rates. Dissociation rates were also easily determined from this data. The binding of dTC to the CM-5/AChBP surface illustrates the use of the AChBP as a molecular biosensor.
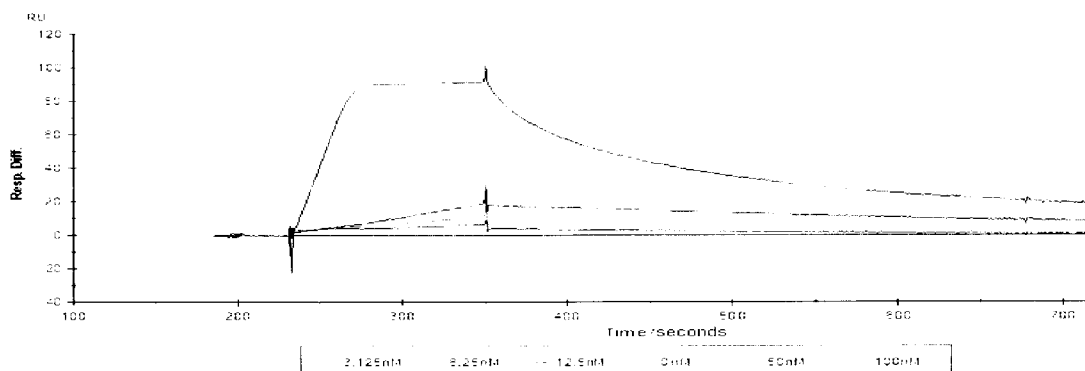
Figure 3.8. Resonance Units (RU) vs. time (seconds) for six concentrations of dTC. Sensor was prepared as described in section 3.2.

Table 3.2 shows preliminary data for SPR experiments. Binding of dTC to AChBP as determined from competition assays is easily accomplished with SPA since it competes for the same binding site as ^{3}H-epibatidine (see table 3.1 above). The data from both assays are comparable (12 nM using SPR and 13 nM using SPA) demonstrating the consistency of the two approaches. For other ligands, such as the nicotinic modulators galanthamine and physostigmine, competition assays are not easily evaluated using radioligand binding since these allosteric modulators exhibit a complex modulatory mechanism that only partially alters binding of ^{3}H-epibatidine. A better approach to this type of ligand would be a label free binding assay such as SPR. Galanthamine and physostigmine were also testing using the SPR approach and the data are also shown in Table 3.2. Their detection on SPR shows one of the unique advantages of this biosensor detection system.

Since this is the first use of SPR with the AChBP, no direct comparison is possible with previous studies; however, dissociation data can be compared to values obtained for these compounds using radioligand binding assays. In addition to dTC, dissociation constants also agree well with functional studies for galanthamine and physostigmine. Our result validates the use of the AChBP as a molecular sensor on SPR surfaces. The two primary advantage of the SPR

technique are 1) It provides association and dissociation data for the test compounds and 2) it provides label free evaluation of binding to any binding site on the protein.

Table 3.2. SPR preliminary data. K_d is the equilibrium binding constant, k_a and k_d are on- and off-rate constants, respectively, Chi2 is a measure of how well the data fits the graph (lower is better). * indicates binding affinity obtained on Aplysia AChBP by inhibition of ^{3}H-strychnine, from Hansen et al [46].

Compound	K_d	k_a (1/Ms)	k_d (1/s)	Chi2	K_d literature	M.W. (g/mol)
d-tubocurarine	12.0 ± 4.1 nM	2.06e9	25.2	5.26	150nM [42]	609.7
Galanthamine	1.6 nM	7.5e4	1.23e-3	15.3	1.5µM*	287.4
Physostigmine	5.7 nM	5.87e3	3.36e-3	0.716	n/a	275.3

3.3.4   Binding of nAChR ligands to AChBP modified MC sensors.

Microcantilevers (MC) represent a novel approach to biosensor applications and are currently in a much earlier state of development then SPA and SPR. They have the advantage of low cost and high sensitivity but currently require more user expertise than other the other two techniques. To investigate the use of the AChBP on microcantilevers, we developed a collaboration with Dr. Hai-feng Ji at Louisiana Tech University in Ruston LA (Dr. Ji has recently relocated to Drexel University, Philadelphia PA).

Scanning electron micrographs of protein immobilized on microcantilevers are shown in figure 3.9 below. Horseradish peroxidase (HRP) and AChBP (not shown) were immobilized on the microcantilever surface using an EDC/NHS crosslinking protocol similar to that used on the SPR surfaces. Methods **A** and **B** differ in the type of surface preparation performed prior to AChBP (or HRP) immobilization. The denser packing apparent in the lower right figure provided an increase in sensitivity to detection of ligand binding to the AChBP. This increase in sensitivity is significant and is an important contribution of Dr. Ji's research.
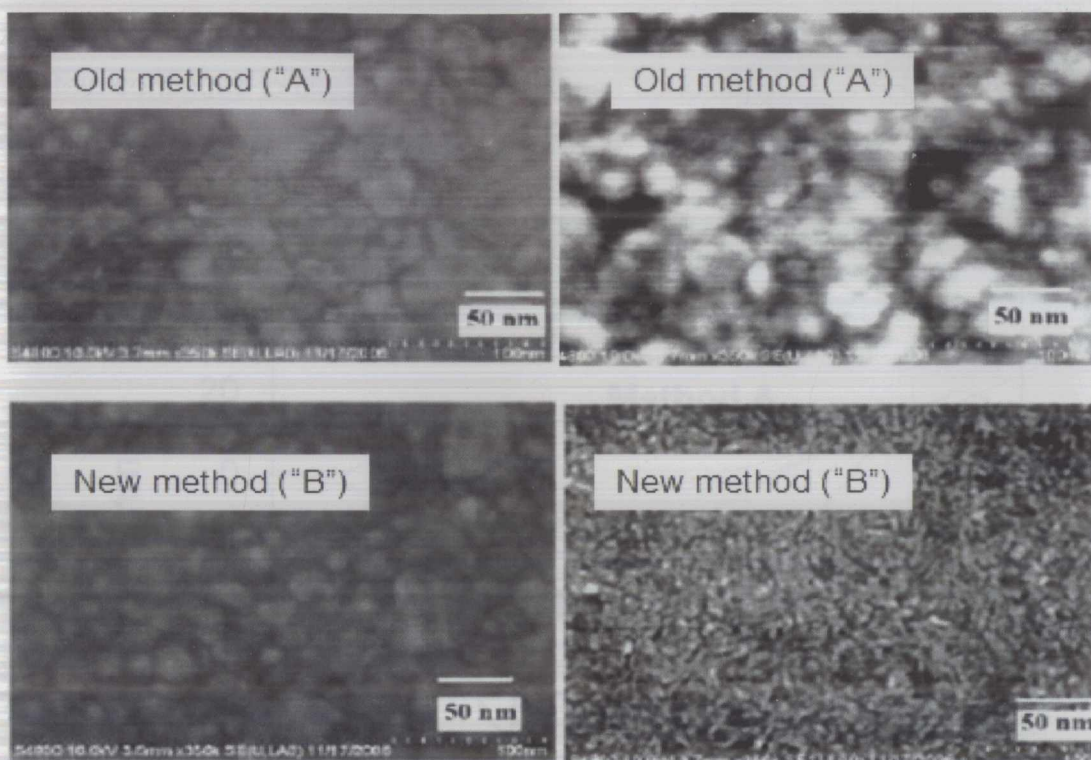
Figure 3.9: SEM images of MC surfaces prepared using two methods. Bottom images show the new method. On the left are images taken before the addition of protein; the difference at this stage is subtle. Note the denser packing with the new method (B) after the addition of protein, at right (Horseradish peroxidase (HRP) in this case- but the effect was the same with AChBP). Images from reference [35].

Figure 3.10 below shows the bending response of AChBP modified microcantilevers in terms of the size of the deflection over exposure time to 10 μM acetylcholine on these two different surface preparations. Method B employed a cleaning protocol to remove particles attached to the microcantilever surface prior to immobilization of analyte protein. The improved preparation method B provides not only an increased sensitivity but better response characteristics; The Langmuir adsorption model produced a better fit of the deflection-time profile of microcantilever B compared to A. The improved bending response afforded by Method B is likely the result of tighter packing of proteins on the microcantilever surface as suggested by the SEM data (Figure 3.9). While it is possible that this close packing of an allosteric protein such as

AChBP might interfere with the proteins function, these data confirm that the protein continues to bind ligand under these conditions.
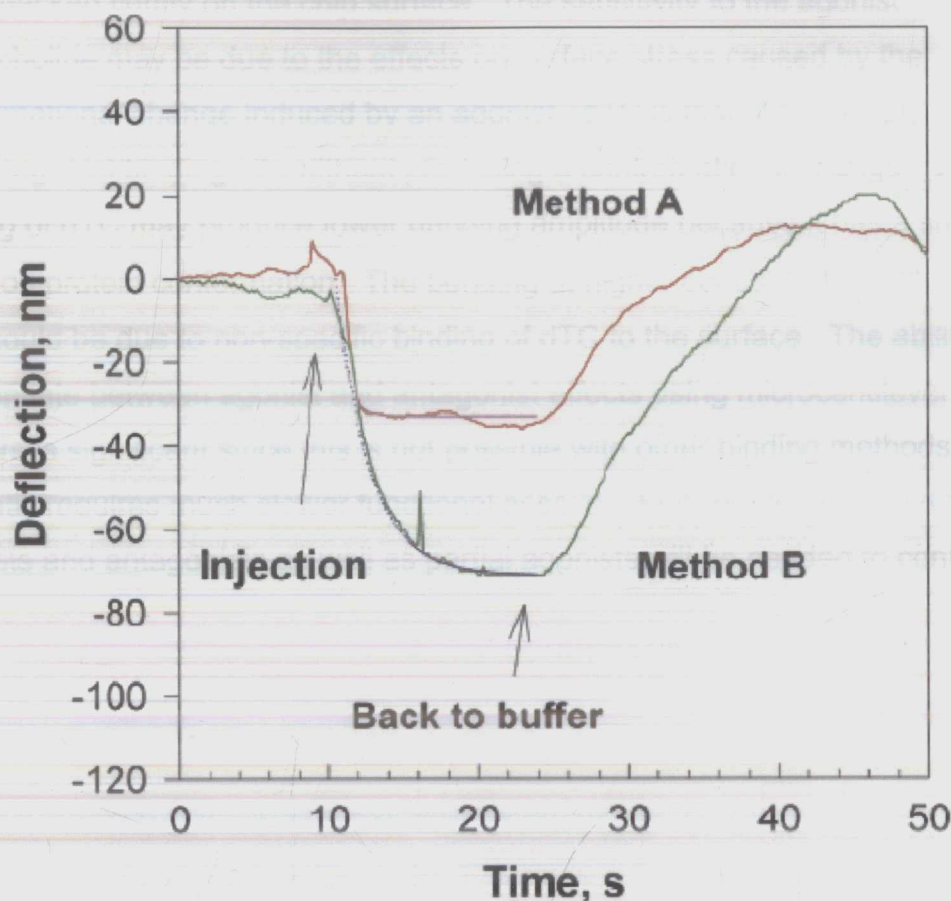
Figure 3.10. Bending response as a function of time. From Gao et al, [35]. Bending response as a function of time of AChBP coated microcantilevers prepared using Methods A and B, on exposure to 10 µM acetylcholine (Ach).

To determine the performance of the AChBP modified microcantilevers in determination of binding kinetics, a concentration series was tested for both the agonist acetylcholine and antagonist dTC. Figure 3.11 shows equilibrium bending of AChBP MC's exposed to acetylcholine (A) and *d*-tubocurarine (B). Acetylcholine produced large bending amplitudes at concentrations near its reported K_d for AChBP binding and a K_d of 4.0 ± 2.4 µM can be estimated from

this data. dTC, in contrast, did not produce large amounts of bending at concentrations near its reported 12 nM K_i value. It has been suggested that proteins undergoing conformational changes produce larger bending amplitudes when packed tightly on the chip surface. The sensitivity to the agonist acetylcholine may be due to the effects on surface stress caused by the conformational change induced by an agonist. dTC is thought to simply compete for the agonist binding site without producing a conformational change. The binding of dTC may produce lower bending amplitude because it has a smaller effect on protein conformation. The bending at higher concentrations (1 μM -1 mM) could be due to non-specific binding of dTC to the surface. The ability to differentiate between agonist and antagonist effects using microcantilever sensors is significant since this is not possible with other binding methods and currently requires much slower functional assays. Further study using different agonists and antagonists as well as partial agonists will be needed to confirm this data.

A. Acetylcholine
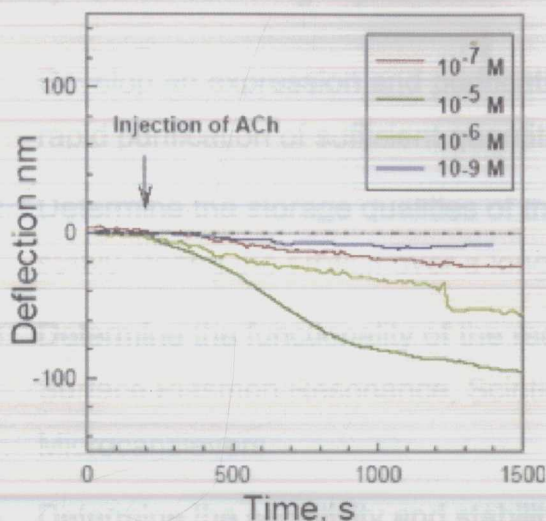
B. *d*-tubocurare
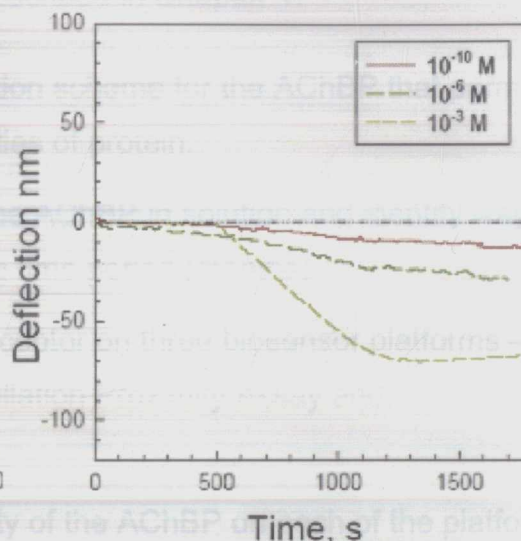
Figure 3.11. Bending response vs. time for AChBP microcantilevers (MC). Analytes acetylcholine and d-tubocurarine (d-tubocurare, dTC) were dissolved in 0.01 M phosphate buffer, pH 7.2 (A and B respectively). The MC's were exposed to the indicated concentrations of analytes. Deflections are as follows. Acetylcholine: 0.001 µM – 12 nm, 0.10 µM – 25 nm, 1.0 µM – 40 nm, 10 µM – 96 nm. dTC: 0.1 nM – 2 nm, 1.0 µM – 21 nm, 1.0 mM, 71 nm.

3.3.4.1 Special acknowledgements for microcantilever assays:

3.4. General Conclusions.

The primary goals of this portion of this thesis were to determine if the AChBP could be attached to biosensor surfaces yet remain active so that binding of ligands can be detected. A secondary goal was to evaluate the

appropriateness of each biosensor platform for different types of ligands. This study had the following objectives as described in Chapter 1:

1. **Develop an expression and purification scheme** for the AChBP that permits rapid purification of sufficient quantities of protein.

2. **Determine the storage qualities of the AChBP** in solution and identify ways of stably storing the protein over a long time period (months).

3. **Determine the functionality** of the receptor on three biosensor platforms – Surface Plasmon Resonance, Scintillation Proximity Assay and Microcantilevers.

4. **Determine the sensitivity and stability** of the AChBP on each of the platforms tested in Objective 3.

The HEK293 expression system described here produced sufficient quantities of the AChBP protein to enable testing of all three target sensor systems. While the expressed protein was a fusion protein composed of an N-terminal Flag epitope tag, the AChBP coding sequence and a C-terminal 6X His sequence, these alterations had no apparent effect on the stability and function of the protein. The protein expressed in a pentameric quaternary structure and binding affinities were similar to previously published AChBP values expressed in the HEK293 cell line. An improvement in the storage and handling of the AChBP protein was the discovery that the protein could be easily dried and reconstituted without lack of activity or alteration in ligand binding.

The AChBP protein was easily immobilized on all three sensor surfaces and performed well in determination of binding kinetics. A comparison of the three sensor surfaces reveals differences in the applicability and sensitivity of each. The SPA assay was the preferred method for evaluation of competitive ligands since it offered low price, no molecular weight limitations and was easily amenable to multiwell plate assays. The quantity of protein required was

extremely low and the results were consistent with previously reported data. The use of a radioligand was the primary disadvantage as well as the requirement that the competing ligand must alter the binding affinity of the radioligand. This second limitation prohibits discovery of novel compounds that may alter receptor function by non-competitive mechanisms.

Protein immobilization on SPR chips using the EDC/NHS method was very successful and now being used by others in the lab to evaluate allosteric ligands on the AChBP. The primary advantages of this method were its ability to detect binding of non-competitive ligands and the potential for screening libraries of non-labelled compounds and natural products and the ability to obtain rate constants for both on and off rates. A serious disadvantage of SPR was its inability to determine kinetics for low molecular weight compounds due to its reliance on molecular weight detection.

The microcantilever experiments suggested a number of intriguing possibilities for high-throughput screening. Although not described in this thesis, Dr. Ji's laboratory is currently working to develop large microcantilever arrays with piezoelectric detection. Our data shows that the AChBP can be used to produce a viable sensor surface using microcantilevers and can potentially be used in this type of arrays to permit rapid screening of multiple receptors at one time. It is this ability to develop an array of receptors that has driven the two projects described in this thesis. By demonstrating the ability of the AChBP modified microcantilevers to detect acetylcholine and to permit determination of accurate binding affinities, we have laid the groundwork for developing these arrays. As discussed in the next chapter, it seems likely that the AChBP can be modified to create proteins with affinities similar to LGIC receptors other than the nAChR. These modified proteins can be added to the detection arrays to permit evaluation of a single drug molecule on multiple receptors simultaneously.

Another significant find in the microcantilever study is the discovery that agonists produce larger bending amplitudes than antagonists. "Conformational-

change based biosensing" would provide a new way to obtain functional data using a chip based, high-throughput system.

Chapter 4: Binding of serotonergic ligands to the AChBP

4.1   Background and Hypotheses.

Chapter 3 discussed the expression, purification and characterization of the AChBP developed in this project. The AChBP was successfully utilized as a biosensor protein using SPA, SPR and microcantilever sensors. While a useful protein for nicotinic ligands, as it currently exists, the AChBP is unlikely to be a useful biosensor for other LGIC ligands. The LGIC family is large and contains at least four different receptor subfamilies including GABA, Glycine and Serotonin in addition to nicotinic acetylcholine receptors. It would be very helpful for drug screening applications if each of these families had a soluble homolog like the AChBP. Unfortunately, no proteins of this type have been discovered. An alternative approach to discovering natural proteins similar to other LGIC receptors is to engineer them using the AChBP as a lead molecule.

As described in Chapter 1, a principal hypothesis of this thesis is that the AChBP can be engineered to selectively recognize different classes of LGIC by mutating key binding site amino acids in the AChBP to corresponding amino acids of the target LGIC receptor.   In this chapter, the interaction of serotonin type 3 receptor (5-HT$_3$R) ligands with the AChBP is investigated.   This is the first step in developing a soluble homolog of the 5-HT$_3$R. No data of this type have been determined previously for the AChBP despite the fact that it was used extensively as a template for generating ligand-docked computer models of the 5-HT$_3$R.

4.1.1. Modelling of LGIC's based on AChBP.

Alignment of the AChBP sequence with the 5-HT$_{3A}$R amino terminal sequence reveals (figure 4.1, [27]) significant sequence similarity (about 20% similarity [22]). Using an alignment similar to figure 4.1 and the crystal structures of the

AChBP, several homology models of the 5-HT$_{3A}$R binding site have been developed [22, 23, 32, 33, 47, 48]. From these models, ligand-docked models have been developed and tested using site-directed mutagenesis. Both antagonist and agonist binding models have been proposed. Antagonist models have focused on the classical 5-HT$_3$R antagonist granisetron and the non-classical antagonist Lerisetron. Agonist models have focused on the full agonist 5-HT and the partial agonist mCPBG (structures in Figure 4.7, section 4.3).

	B-Loop (mouse5-HT$_{3A}$R S182-I190)		C-Loop: (m5-HT$_{3A}$R, E225-M237)
AChBP	R I K I G S W T H H S R E I		S V T Y S C C P E A Y E D V
m5-HT$_{3A}$R	S L T F T S W L H T I Q D I		E - F S I D I S N S Y A E M
h5-HT$_{3A}$R	(Identical to mouse)		E - F S M E S S N S Y A E M

	D-Loop: (m5-HT$_{3A}$R, T86 – W102)		E-Loop: (m5-HT$_{3A}$R, Y141 – Y153)
AChBP	D V V F W Q Q T T W S D R T L A W		- P Q L A R V V S D G E V L Y M
m5-HT$_{3A}$R	T T Y I W Y R Q Y W T D E F L Q W		Y - - - V Y V H H R G E V Q N Y
h5-HT$_{3A}$R	(Identical to mouse)		Y - - - V Y I R H Q G E V Q N Y

	A-loop: (mouse 5-HT$_{3A}$R 114-130)		F-loop: (mouse 5-HT$_{3A}$R 195-212)
AChBP	S V P I S S L W V P D L A A Y N -		- S V D P T T E N S D D S E Y F S Q Y S
m5-HT$_{3A}$R	S I P T D S I W V P D I L I N E F		W – R S P E E V R S D K S I F I N Q - G
h5-HT$_{3A}$R	(Identical to mouse)		W - R L P E K V K S D R S V F M N Q - G

Figure 4.1: Sequence alignment of binding loops in AChBP and 5-HT$_{3A}$R's.
Aligned sequences: LS AChBP, murine 5-HT$_{3A}$R (m5-HT$_{3A}$R) [33], and human 5-HT$_{3A}$R (h5-HT$_{3A}$R)[27]. The underlined amino acid residues indicate their significance (mutations to alanine have a ten-fold or more effect on binding) for binding to agonist (blue), antagonist (red), lerisetron + agonist (purple) & agonist + antagonist (green). Note that colored residues in the B-loop, D-loop and F-loop may be important to agonists and lerisetron as well as antagonists, but data to this effect is not available.

4.1.2. Binding models for the 5-HT$_{3A}$R antagonist granisetron.

Several recent models describing binding of granisetron to the 5-HT$_{3A}$R have been proposed by the labs and collaborators of Sarah Lummis [13, 32, 33, 49] and Marvin Schulte [22, 23, 48]. In the majority of the recent models from both groups [22, 49] granisetron docks within 4-5 Å of both Y234 and W183 (see figure 4.2). Some part of granisetron is typically (except in one of the Lummis

models) docked between the superficially-located C-loop Y234, and the deeper B loop W183. Residues W90, Y153 and D229, which also seem to be involved in binding granisetron, are also within 4-5 Å of granisetron in most of the models. In each of the models, granisetron lies adjacent and parallel to the backbone of the B-loop of the primary (+) face, with the C-loop forming something like an open "lid" as mentioned earlier.

The Lummis models [49] were divided into three classes, which together placed a total of 26 residues close (≤5 Å) to granisetron, of which 8 were common to each of the models. Of these 8, W90 (D-loop, complementary (-) face) and T179 (B-loop, (+) face) are probably important to binding granisetron, according to mutagenesis studies. Two groups of Lummis models (termed A and B) have either the azobicyclic structure (group A) or the aromatic rings (group B), of granisetron situated between critical aromatic residues W183 and Y234. Group C models place granisetron close to several F-loop residues but not close to W183 or Y234, but perpendicular to the B-loop. Group C models were tentatively ruled out by the authors based on lack of support by mutagenesis data. The evidence presented for model group B (the authors' favourite) over model group A is not convincing (Y153 hydrogen bonding is implicated, and previous research is sited, but the Y153F mutation which the authors tested indicates that Y153 plays its role possibly partly via its aromatic ring).

Joshi et al. [22] investigated the binding (docking) of granisetron to an agonist-free (lid-open) model of the 5-HT$_{3A}$R, which utilized the recently-obtained high-resolution nAChR structure by Unwin et.al [5]. The authors indicated two separate sets of binding sites for this molecule, and both appear to be important. The first, "B" position (in one of two orientations - B1 or B2) orientations), acts as a pre-docking site, and the second "A" position (in either of two orientations - A1 or A2) is the final high affinity binding site for granisetron. The two-site theory was adopted because granisetron is not long enough to bind to residues in two regions of the receptor determined by mutagenesis as critical to ^{3}H-granisetron

binding at the same time (see section 4.3, figure 4.6 for structure of granisetron). Like in the Lummis models, these models have either the azobicyclic structure (orientation B1 and A2) or the aromatic rings (orientation B2 and A1), of granisetron situated between critical aromatic residues W183 and Y234 (in other words, deep from loop C). ^{3}H-granisetron is thought to pre-dock utilizing residues H185, D189, L184 and possibly W183 then move into the final high affinity site where it is postulated to utilize interactions to W90, W183, Y234, D229 and E129. Of these residues, W183, H185, Y234 and D229 are thought to be most important.

"Up" to extracellular

"Down" to membrane

C: Y234 (Y)

B: W183 (W)

A: E129 (N)

E: Y143 (R)
E: Y141 (L)
E: Y153 (M)

D: W90 (W)

F: R196 (V)
F: D204 (D)
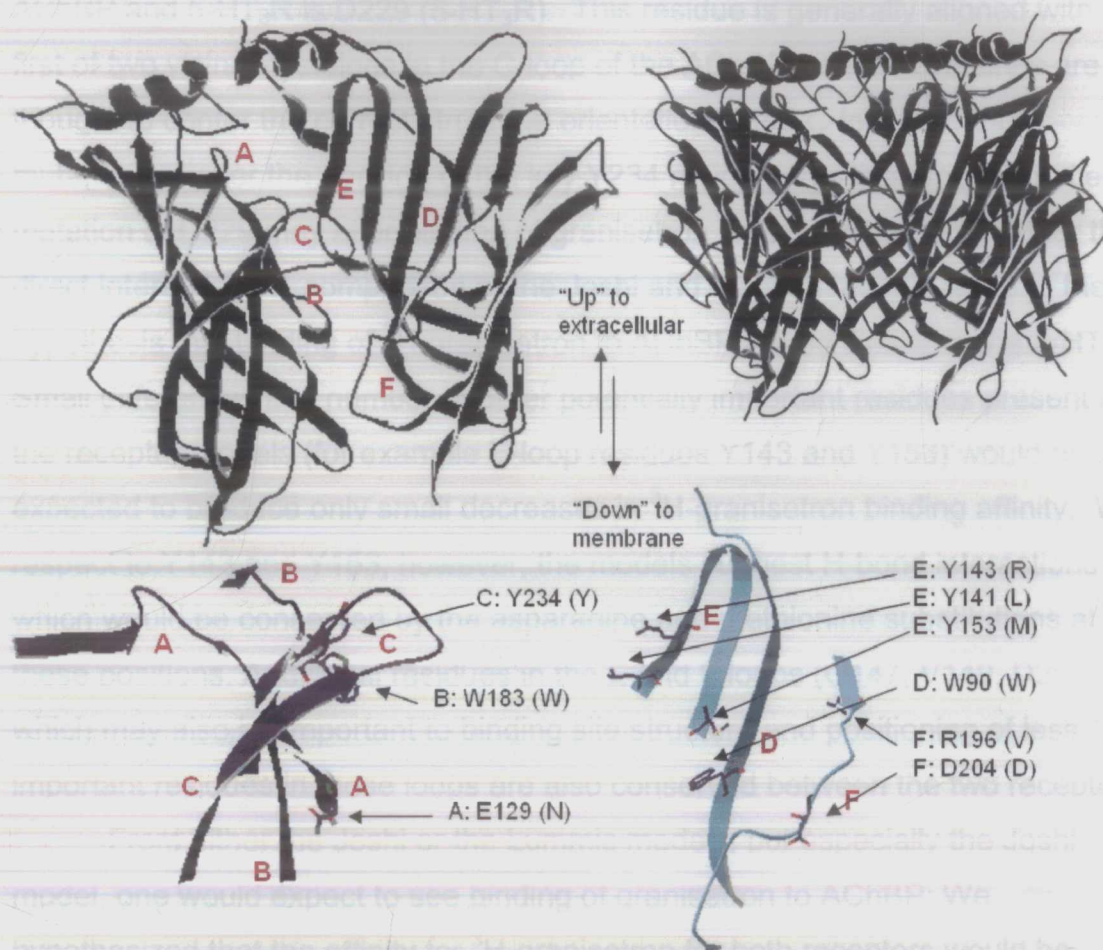
Figure 4.2. Conserved structural features of the binding sites. These pictures are derived from crystal structure of AChBP (PDB entry 1I9B [27]) using DeepView. Upper right: Side view of the AChBP pentamer. Upper left: the binding cleft is formed by two adjacent subunits. Loops A-F are named in red. Bottom: everything is removed except the binding loops A-F, for clarity. The figure on the lower right would be deep to the figure on the lower left, as indicated by the upper left figure. Arrows indicate the side chain positions where side chains are shown, and AChBP residues are given in parentheses- example "E: Y143 (R)" means binding loop E, 5-HT$_{3A}$R position of Y143, AChBP residue is arginine (R).

Of the key residues implicated in the Lummis and Joshi models, W183 and H185 in the B-loop, Y234 in the C-loop and W90 in the E loop are all conserved in the AChBP. H185 in the Joshi model is also conserved and only a moderate substitution at D189 is present in the AChBP (E- Glutamate). Thus all of the key residues thought to interact with granisetron in the 5-HT$_3$R are conserved in the AChBP. The primary difference in key residues between the

AChBP and 5-HT$_3$R is D229 (5-HT$_3$R). This residue is generally aligned with the first of two vicinal cysteines in the C-loop of the AChBP. These cysteines are thought to confer the correct structural orientation of the C-loop and thus mutation will alter the position of the key Y234 residue. In mutagenesis studies, mutation of D229 may alter binding of granisetron via a structural role rather than direct interaction. A comparison of the Joshi and Lummis models leads to the hypothesis that binding of ^{3}H-granisetron to AChBP will be similar to the 5-HT$_3$R. Small differences in a number of other potentially important residues present in the receptor models (for example E-loop residues Y143 and Y153) would be expected to produce only small decreases in ^{3}H-granisetron binding affinity. With respect to Y143 and Y153, however, the models suggest H-bond interactions which would be conserved by the asparagine and methionine substitutions at these positions. Additional residues in the E and F loops (G147, V149, D204) which may also be important to binding site structure and positioning of less important residues in those loops are also conserved between the two receptors.

From either the Joshi or the Lummis models, but especially the Joshi model, one would expect to see binding of granisetron to AChBP; We hypothesized that the affinity for ^{3}H-granisetron for both receptors would be similar based on the conservation of residues W90, W183, Y234, and their importance to granisetron binding in both sets of models. It is possible, of course, that a lack of conservation in a few less-critical residues could produce slightly weaker binding to the AChBP. Structural similarity of granisetron and other classical 5-HT$_3$R antagonists would suggest that MDL72222 and tropisetron would also bind to the 5-HT$_{3A}$R with similar affinities.

4.1.3. Binding models for 5-HT$_{3A}$R agonists 5-HT and *m*CPBG.

Alanine scanning mutagenesis has implicated the tyrosine residues Y143 and Y153 in the E-loop, [50], F226 in the C-loop [23], and T179 and F180 in the B-loop [47] of the murine 5-HT$_{3AS}$R, as particularly important to binding of 5-

HT$_3$R agonists. Alanine mutants at these positions result in at least a one hundred-fold decreases in agonist affinity, but only tenfold or less decrease in antagonist affinity. Selectivity of some mutations for full versus partial agonists have also been observed. Alanine mutations of I228 and D229 (C-loop) decrease binding affinity of the 5-HT$_{3A}$R for 5-HT, but not mCPBG. Y234F mutation of the 5-HT$_{3A}$R results in 125- and 185-fold decreases in mCPBG or 5-HT (agonist) binding respectively, but only an 11-fold decrease in ^{3}H-granisetron binding. In addition to these agonist selective residues, several of those mentioned above for antagonists (Section 4.1.2) are also important to agonist binding and/or gating [47].

Reeves et al. [32] first used homology modelling based on AChBP (from the HEPES-bound AChBP crystal structure, [27]) to probe the docking of 5-HT to the 5-HT$_{3A}$R. Seven energetically favourable models were described. In three of these, the primary amine of 5-HT is situated in the lower (proximal to the membrane) part of the binding cleft, near W90, and the aromatic part is "sandwiched" between B-loop's W183 and C-loop's Y234 aromatic rings. The hydroxyl group of 5-HT appears in these first three models to be in a hydrophilic pocket formed by R92, Q151, and D229. In the fourth and fifth models, the primary amine of 5-HT is between W183 and Y234, the aromatic rings are in the lower part of the cleft, and the hydroxyl group is in a hydrophilic pocket formed by T179, E236, and N128. In these first five models, either the indole nitrogen-bound hydrogens (in models 1-3), or the primary amine hydrogens (models 4-5) form hydrogen bonds with the exposed S182 backbone carbonyl oxygen, so that the 5-HT nitrogens line up vertically along the B-loop, leaving the six-membered ring pointing right (models 1-3) or left (models 4-5). In the sixth and seventh models, the indole nitrogen is located toward the top of the cleft, but the primary amine is pointed toward the right (minus-face side) in model six, or left (model seven). In addition to those residues above, Y143 and Y153 can form hydrogen

bonds of various lengths (most of which are fairly long, however) with 5-HT. The authors chose model 4.

More recently, Suryanarayanan et al [23] developed ligand-docked models for 5-HT, 2-Methyl-5-hydroxytryptamine (2-Me-5-HT), and *m*-Chlorophenylbiguanide (*m*CPBG) binding to the 5-HT$_{3A}$R; also using a homology model based on Brejc et al [27]. A single binding orientation was determined for 5-HT from these studies. 2-Me-5-HT bound in a similar orientation to 5-HT. Two modes of binding were determined for *m*CPBG, one which placed *m*CPBG in a different orientation from that of 5-HT (*m*CPBG model 1), and one where the orientation was nearly the same as for 5-HT (*m*CPBG model 2). In the 5-HT model and *m*CPBG model 2, the primary amino and guanidino groups of 5-HT and *m*CPBG respectively are intercalated between F226 and Y234 in the C-loop, and forms a salt bridge with E236. The aromatic group ring of 5-HT is involved in π-π interactions with W183, while the hydroxyl group hydrogen bonds with D229. Y153 was found to be close (within 4 Å) to 5-HT in this as well as the Reeves et al models, and can form cation-π or hydrogen bond interactions with the guanidino group in *m*CPBG model 1.

It should be noted that the AChBP crystal structure, upon which these agonist-binding models was based, is thought to resemble the closed-desensitized state rather then the open state of the 5-HT$_{3A}$R. The desensitized state is thought to have a higher affinity for agonists than the open state. Since the true structural differences between open and desensitized states are unknown, models based on desensitized state binding may include structural errors.

A key receptor region in both binding of agonists and conformational change in the 5-HT$_3$R is the C-loop. This region is thought to close over the agonist prior to channel opening. The C-loop region is highly variable between LGIC receptors that bind different classes of agonists. Since this is a highly variable region with little sequence homology between the AChBP and 5-HT$_3$R,

the C-loop sequences of the 5-HT$_{3A}$R and AChBP are difficult to align. This places doubts on the structural/functional equivalency of AChBP residues to 5-HT$_{3A}$R residues in this loop. It is true that the alignment shows great dissimilarity between human 5-HT$_{3A}$R residues and AChBP residues in this loop, but there is also a lack of conservation between the 5-HT$_{3A}$R's of human and mouse. It has been proposed [22] that the C-loop of the 5-HT$_{3A}$R forms a "lid" which closes ("lid-shut") over agonists during binding, but stays open during binding to antagonists. Likely, then, a functional characteristic of an agonist is to induce the closing of this lid, and the closing of the lid is linked to the activated (channel open) state of the receptor. A closed lid would allow more interactions of agonists with the C-loop of the receptor, which accounts for mutagenesis and modelling data that implicate C-loop residues F226, I228, D229, and E236 (there is no mutagenesis data available to indicate the importance or lack thereof of E236) in binding the agonist 5-HT, but not granisetron.

The above C-loop residues are not conserved in AChBP. Neither are the critical E loop tyrosines Y143 and Y153, although a small shift in the AChBP alignment would allow for a nearby tyrosine to align with Y153. 5-HT$_{3A}$R Y234 appears to be conserved, however, and E236 aligns with an aspartate (D) in AChBP. Because of the conserved B-loop residues mentioned above, it could be expected that 5-HT$_{3A}$R agonists would bind to AChBP, but much more weakly than antagonists would.

4.1.4. Binding models for the 5-HT$_{3A}$R antagonist lerisetron.

Lerisetron is structurally different than the other 5-HT$_{3A}$R antagonists studied here in that it has a benzyl group protruding sideways from its aromatic part, it has no carbonyl oxygen, and it has a piperazine group instead of an azobicyclic group. Although it is often considered a special class of serotonergic antagonist, it does contain the basic antagonist pharmacophore: aromatic on one end, and an amine base on the other separated by a distance of about 9 Å.

Mutagenesis studies indicate that the E-loop tyrosines Y143 and Y153 on the 5-HT$_{3A}$R are critical to its binding lerisetron [50]. From these mutational studies and a comparison of the granisetron and lerisetron structures, it might be expected that lerisetron would bind AChBP with an affinity somewhere between that of serotonergic agonists and classical antagonists.

4.1.5. Summary

Analysis of 5-HT$_3$R data and ligand-docked homology models in comparison to the AChBP crystal structure data suggests that serotonergic agonists and antagonists will interact quite differently with the AChBP. We hypothesized that the serotonin antagonists granisetron, MDL-2222 and perhaps lerisetron would bind with high affinity to the AChBP, although possibly 10-100 fold less tightly than to the 5-HT$_3$R due to small substitutions of some interacting or structurally relevant amino acids. Serotonergic agonists, however, are expected to bind with much lower affinity at the AChBP due to large sequence dissimilarities between the AChBP and 5-HT$_3$R in regions postulated to be critical binding areas for these ligands; particularly the C-loop and E-loop regions. In order to test these hypotheses, we evaluated the interaction of a series of serotonin agonists and antagonists with the AChBP. Our data largely support our hypotheses; however, the non-classical antagonist lerisetron was found to bind much more weakly than classical antagonists to the AChBP. These data provide insight into the reliability of ligand-docked models of the receptors and provide information for use in developing a serotonin binding protein.

4.2   Methods.

We used scintillation proximity assay to evaluate the binding of serotonin type 3 receptor (5-HT$_3$R) agonists, partial agonists and antagonists to the AChBP. We expressed an AChBP fusion protein containing a 6X Histidine tag on

the C-terminal, and a 3XFlag tag on the N-terminal under control of a CMV promoter. The sequence of the AChBP was determined from published reports and synthesized using commercial DNA synthesis. His and Flag tags were added to facilitate an affinity purification scheme as previously described. The protein was expressed in HEK 293 cells, and purified on Sigma His-Select nickel-EDTA columns. Chapter 3 of this thesis described this expression and purification and demonstrated the integrity of the expressed protein. Validation of the binding kinetics of this AChBP were also determined in experiments described in Chapter 3 and found in agreement with previously published data from cloned AChBP protein obtained from *Lymnaea stagnalis*.

SPA differs from conventional binding assays in that no filtering is required to separate bound and unbound ligand. This makes the procedure easier to automate and produces highly consistent results in a small amount of time. The primary drawback of the technique is the need for a radiolabelled ligand. Since radioligands are not available for all of the compounds evaluated here, experiments to determine the affinity for non-labelled compounds utilized competition assays. Typically ^{3}H-epibatidine was used as the radioligand in these experiments.

4.2.1 Binding of ^{3}H-epibatidine and ^{3}H-granisetron to AChBP.

For ^{3}H-epibatidine radioligand binding, a suspension of 0.1 mg beads per ml in phosphate buffered saline (PBS, see appendix 2), was incubated one hour with 2 mg/ml BSA, and 0.0125 nM AChBP. Three ml of this suspension was added to 4ml scintillation vials. Seven concentrations of ^{3}H-epibatidine were used with concentrations increasing in three-fold steps from 0.004 nM to 3.0 nM. Control tubes containing no ^{3}H-epibatidine were also included. Samples were capped and shaken for one minute then equilibrated for one hour at room temperature before counting. Typical B_{max} values of 1000 counts per minute

(CPM) were obtained, with a percent error of about 5%. The ^{3}H-epibatidine binding curve is shown in figure 4.3.
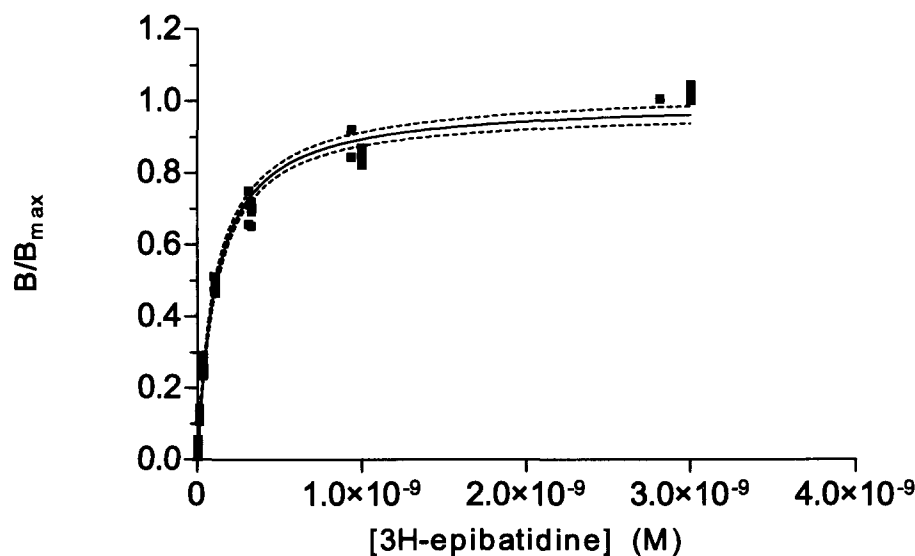
Figure 4.3: Binding of ^{3}H-epibatidine to AChBP. Dashed lines represent 95% confidence interval (95% CI). Data shown were obtained by 7 different experiments using different preparations of AChBP.

For ^{3}H-granisetron binding the binding assay was modified to use a higher concentration of protein (2.6 nM AChBP) due to the expected lower affinity of ^{3}H-granesetron. Only 200 μl of beads/radioligand mix were required per sample. ^{3}H-granisetron concentrations were varied between about 1.0 nM and 240 nM. Nonspecific binding was determined in the presence of 1.0 M acetylcholine, and was subtracted. Incubation time was increased to at least two hours.

4.2.2 Competition assays.

^{3}H-epibatidine (1.0 nM) was used as the radioligand in competitive binding experiments, with 0.025 nM AChBP, in 3 ml. Inhibitor concentrations ranged from 9- fold below the expected Ki to 9- fold above and were varied in 3-fold steps. Initial scouting, to estimate K_i values, used 10-fold steps in concentration

beginning with 0.10 nM and increasing until the binding of (1.0 nM) ^{3}H-epibatidine was either maximally inhibited or the concentration exceeded 1mM. Care was taken so that bound radioligand remained ≤10% of total ligand added. Final ligand concentration was calculated as Initial concentration - bound ligand. Competing ligand was added before the radioligand, and the mixture equilibrated for at least two hours prior to counting.

4.2.3 SPA data analysis.

Data were analyzed using Graph Pad Prism 4.0 software. The K_d values for ^{3}H-Epibatidine and ^{3}H-granisetron were calculated using the simple one-site binding model:

Equation 1 $Y/B_{max} = X / K_d + X,$

where X is radioligand concentration and Y is the fraction bound (measured as s counts per minute. For ^{3}H-epibatidine, non-specific binding signal was <<10%, and was ignored. Non-specific binding of ^{3}H-granisetron was linear with ligand concentration, and was determined in parallel experiments and subtracted.

For competition experiments, the fractional response remaining at each concentration of competing ligand was plotted against the ligand concentration. An IC_{50} value was determined from this data using Graphpad prism software and the following equation:

Equation 2 $Y = 1 / (1 + 10^{([\log(IC50)-X] * \text{Hill slope})})$

where X is the logarithm of the molar concentration of inhibitor ligand, and Y is fraction bound at a specific inhibitor concentration. An apparent K_i was calculated from the IC50 using the Cheng-Prusoff relation: $K_i = IC_{50} * (K_{d(epi)}/[epi])$.

4.3   Results

Serotonin (5-HT), *m*-chlorophenylbiguanide (*m*CPBG), 2-methyl-serotonin (2-Me-5-HT), phenylbiguanide (PBG), lerisetron, MDL72222, and tropisetron all competed with epibatidine for the primary binding site on AChBP, binding with affinities (K_i) ranging from 33 nM for the 5-HT$_3$R antagonist tropisetron to 600 μM for PBG. ^{3}H-Granisetron, which is structurally similar to tropisetron and can be inhibited by either MDL72222 or acetylcholine (data not shown), can therefore now also be assumed to bind to the primary AChBP site, bound with a K_d of 21.7 nM (Figure 4.4, Table 4.1.). Table 4.1 (section 4.3.1) also compares the affinities acquired for the AChBP with literature values of the same compounds binding to the murine 5-HT$_{3AS}$R.

4.3.1   Binding of 5-HT$_3$R antagonists to AChBP.

Since granisetron is available in a radio-labelled form (^{3}H-granisetron), binding could be determined directly. Figure 4.4 below shows binding of ^{3}H-granisetron to AChBP-bound SPA beads. The apparent K_d for granisetron binding was determined to be 22 ± 1.4 nM. This is about 20 fold less than its affinity on 5-HT$_3$Rs (1.0 ± 0.16 nM) and is within the range predicted by our analysis of the mutagenesis and structural data.
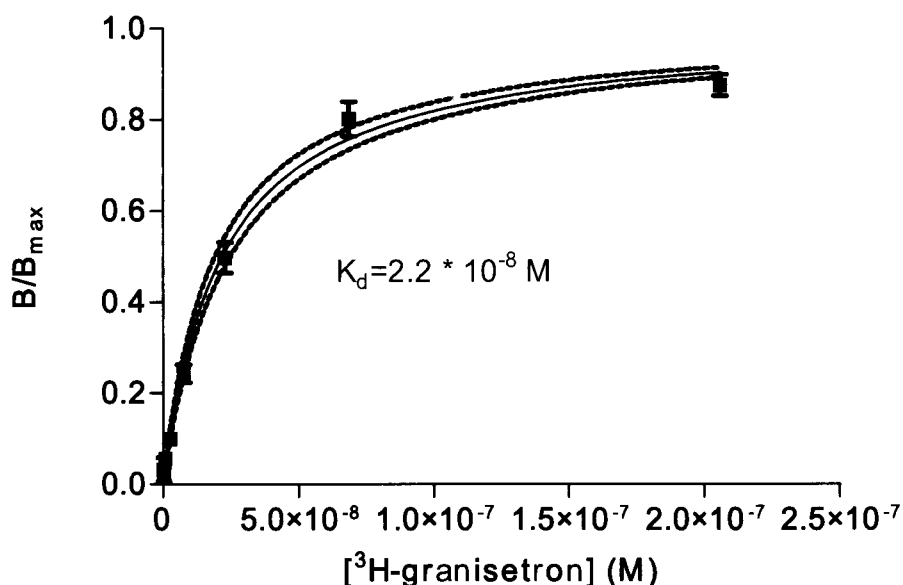
Figure 4.4: ^{3}H-granisetron binding to AChBP. ^{3}H-granisetron binding was determined by exposing AChBP bound SPA beads to increasing concentrations of ligand. Non-specific binding was subtracted from total binding to obtain this data. Data from 4 experiments were fit to a one site binding model using non-linear regression and Graphpad Prism software. Dashed lines indicate the 95% confidence intervals. The data represent pooled data from four independent experiments.

Results of competition studies with other 5-HT$_3$R antagonists are shown in Figure 4.5 and summarized in Table 4.1. These data reveal differences in binding of tropisetron, MDL-72222 and d-tubocurarine similar to those observed for ^{3}H-granisetron. Tropisetron binds about 30 fold weaker on the AChBP compared to its affinity for the 5-HT$_3$R. MDL-72222 binds about 3.5 times weaker and d-tubocurarine only 2 fold weaker. Granisetron, MDL-72222 and tropisetron are considered part of the same structural family as granisetron and this data is consistent with our hypothesis (see figure 4.6 for structures). d-tubocurarine, although a different structural class is thought to utilize an aromatic-amino group pair of interactions similar to granisetron and so may be binding to a very similar group of amino acids.
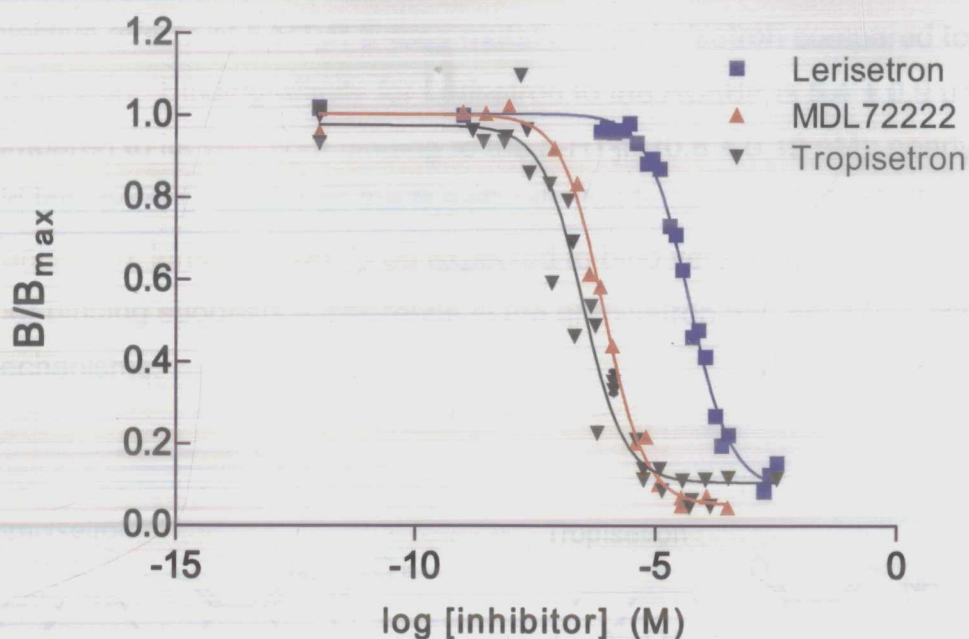
Figure 4.5: Inhibition of ^{3}H-Epibatadine binding to AChBP by 5-HT$_3$R antagonists. Data represent pooled results from 3 experiments. K$_i$ values for compounds are as follows: tropisetron 33 ± 10 nM, MDL72222 92 ± 20 nM, and Lerisetron 5400 ± 900 nM.

Table 4.1: Serotonergic antagonist binding to AChBP and 5-HT$_3$R.
K$_d$ and K$_i$ data for AChBP (2nd column) were determined in at least three replicate experiments. 5-HT$_3$R data (3rd column) are literature values obtained using murine serotonin type 3A and 3AS receptors. Relative affinities (fourth column) indicate the affinity on the AChBP relative to the 5-HT$_3$R data in column 3 and were calculated by dividing column 3 by column 2.

Compound	K$_d$ or K$_i$ ± SE (From this study)	5-HT$_3$R K$_d$ or K$_i$ ± SE (From Previous Studies)	AChBP K$_i$/ 5-HT$_3$R K$_i$
Granisetron	22 ± 1.4nM (K$_d$)	0.96 ± 0.16 nM	23
Tropisetron	33 ± 10 nM	1.1 nM	30
MDL72222	92 ± 20 nM	27 nM	3.4
Lerisetron	5.4 ± 0.9 µM	0.8 ± 0.19 nM	6700
d-tubocurarine	14 ± 0.2 nM	6 ± 2 nM	2.3

Lerisetron is a non-classical antagonist for the 5-HT$_3$R that contains structural features not found on classical agonists; namely the addition of a

second aromatic group (Figure 4.6, below) Mutagenesis studies have indicated selective effects of 5-HT$_3$R E-loop mutations on lerisetron compared to granisetron. Binding affinity for Lerisetron to the AChBP is 5.4 ± 0.9 µM compared to its very tight binding to the 5-HT$_3$R (0.8 ± 0.19 nM); nearly 7000-fold less potent. Based on the hypothesis that lerisetron binds similarly to granisetron, lerisetron would be expected to bind very tightly to the AChBP. The poor binding suggests a difference in the granisetron and lerisetron binding mechanisms.

Granisetron

Tropisetron

MDL72222

Lerisetron
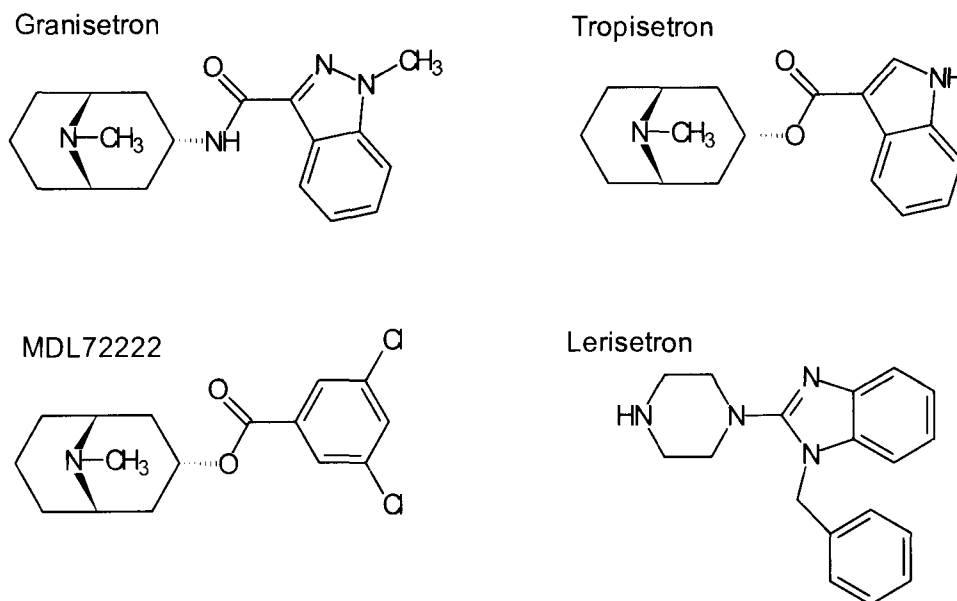
Figure 4.6. Structures of the 5-HT3R antagonists in this study. Note that the amine nitrogens are basic and should be considered positively charged at pH 7, although this is usually not indicated, and is not indicated in the figure. Figure made using ChemWindow.

4.3.2 Binding of 5-HT$_3$R agonists to the AChBP.

Serotonin (5-HT), 2-methyl-5-hydroxytryptamine (2-Me-5-HT), *m*-chlorophenylbiguanide (*m*CPBG) and phenylbiguanide (PBG) represent two groups of agonists/partial agonists for the 5-HT$_3$R (See figure 4.7 for agonist

structures). The rank efficacy for all 4 agonists is: Serotonin>*m*CPBG>PBG>2-Me-5-HT. Agonists for the 5-HT$_3$R occupy a binding site that overlaps the antagonist binding domain thus agonists and agonists compete for binding to the receptor. A fundamental difference between agonist and antagonists is thought to be the ability of agonists to interact with the C-loop causing it to rotate down and "cap" the binding site. The open conformation (C-loop rotated out) is often termed the "lid open" conformation and the closed conformation (C-loop rotated down) the "lid closed" conformation. These terms should not be confused with the "open" and "closed" conformations of the integral ion channel. Rotation of the C-loop down to the lid closed conformation ultimately leads to channel opening. The movement of the C-loop to the closed position typically produces a higher affinity binding site for the agonist/partial agonist.
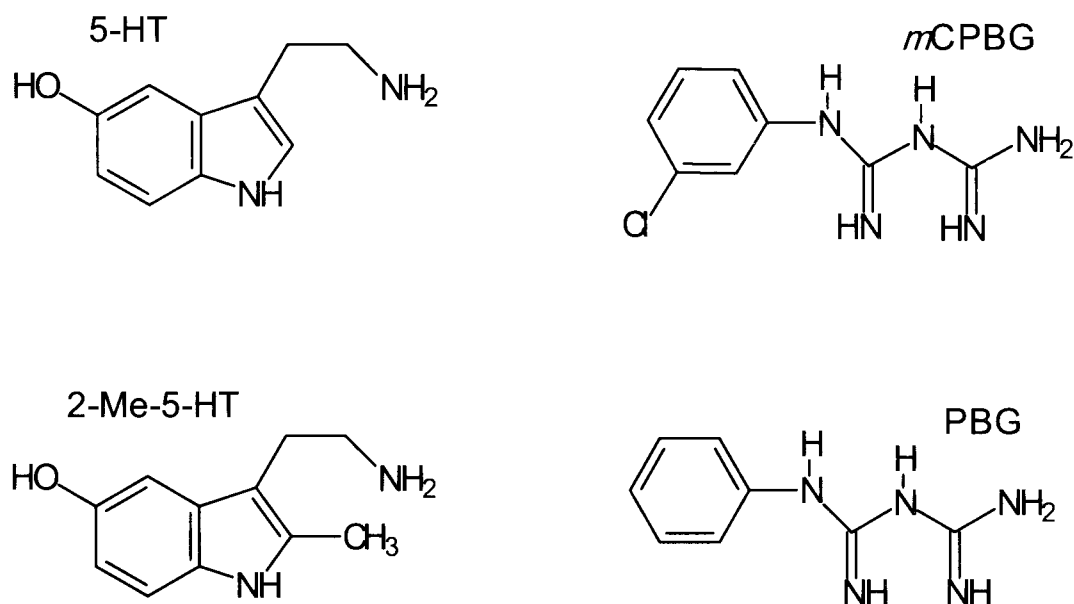
Figure 4.7. Structures of the 5-HT$_3$R agonists in this study. Abbreviations are 5-HT, serotonin; 2-Me-5-HT, 2-Methyl-serotonin; *m*CPBG, *m*-chlorophenylbiguanide; and PBG, phenylbiguanide. Note that the amine nitrogens are basic and should be considered positively charged at pH 7, although this is usually not indicated, and is not indicated in the figure. Figure made using ChemWindow.

As discussed earlier, we hypothesize that agonists will bind significantly more weakly to the AChBP due to differences between the AChBP and 5-HT$_3$R sequences, primarily in C-loop residues (although other residues are also involved). To test this hypothesis, we evaluated 4 different 5-HT$_3$R agonists (shown in figure 4.8 and tabulated in Table 4.2.)
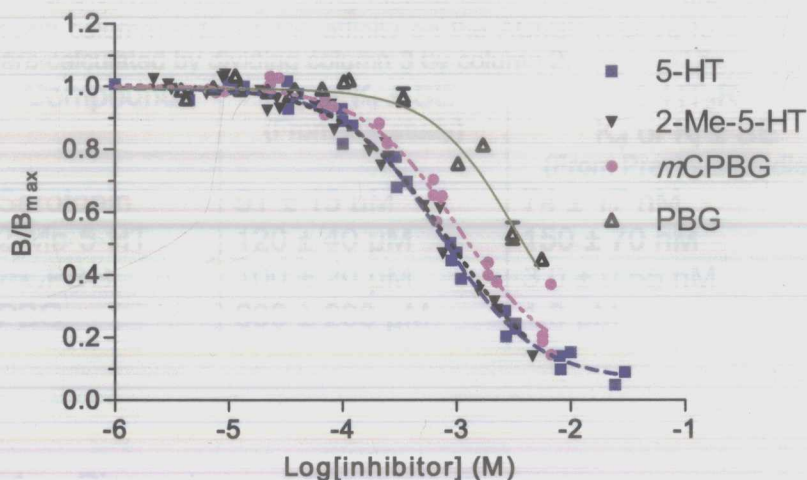
Figure 4.8. Inhibition of ^{3}H-Epibatadine binding to AChBP by 5-HT$_3$R agonists. Normalized data points from 3 experiments are plotted on a single graph and fit to a one-site competition model (See materials and methods).

Rank potencies for the 4 agonists tested were significantly different on the AChBP compared to the 5-HT$_3$R (Table 4.2). On the 5-HT$_3$R, rank potencies are: mCPBG > 5-HT > 2-Me-5-HT > PBG. For the AChBP, 5-HT, 2-Me-5-HT and mCPBG were essentially identical in affinity with PBG about 6 fold less potent than the other three. This change in rank potencies was reflected in the relative affinities on AChBP versus 5-HT$_3$R (Table 4.2). The largest differences were observed for mCPBG which was 33,000 fold less potent on the AChBP. 5-HT and 2-Me-5-HT were similar and PBG was the least effected. This weaker binding is consistent with our hypothesis that large structural changes in the C-

loop region may produce significant differences in binding affinity for agonists. The extremely large difference in binding of *m*CPBG compared to PBG is somewhat surprising although it should be noted that the PBG is a far weaker partial agonist than *m*CPBG.

Table 4.2. 5-HT$_3$R agonists binding to the AChBP and 5-HT$_3$R. K$_d$ and K$_i$ data for AChBP (2nd column) were determined in at least three replicate experiments. 5-HT$_3$R data (3rd column) are literature values obtained using murine serotonin type 3A and 3AS receptors. Relative affinities (fourth column) indicate the affinity on the AChBP relative to the 5-HT$_3$R data in column 3 and were calculated by dividing column 3 by column 2.

Compound	K$_d$ or K$_i$ ± SE (From this study)	5-HT$_3$R K$_d$ or K$_i$ ± SE (From Previous Studies)	AChBP K$_i$/ 5-HT$_3$R K$_i$
Serotonin	91 ± 15 µM	74 ± 17 nM,	1200
2-Me-5-HT	120 ± 40 µM	150 ± 70 nM	800
*m*CPBG	100 ± 20 µM	3.0 ± 0.55 nM	33,000
PBG	600 ± 200 µM	1.3 µM	460

4.4   Discussion and Conclusions.

As we expected, all of the serotonergic ligands tested bound to 5-HT$_3$R with higher affinity than to AChBP. However there were some important differences. This section discusses these differences and analyzes the 5-HT$_3$R models.

4.4.1 Antagonist versus Agonist differences.

In general, 5-HT$_3$R antagonists tend to have considerably higher affinity for the AChBP than the agonists (Table 4.1 and 4.2) In fact, antagonist affinities are reasonably close to the corresponding 5-HT$_3$R affinities. This result is convincing evidence for the validity of 5-HT$_3$R antagonist binding models based on AChBP (particularly those from the Lummis and Schulte labs). These results support the proposed role of the highly conserved residues in the B and D binding loops of the 5HT$_3$R in binding antagonists. The E and C-loops which

show differences between the two binding sites are likely to be responsible for the large difference between agonist and antagonist binding. Due to the significant structural difference between the C loops of the two receptors, it is likely that this loop is primarily responsible for the difference in comparative binding affinities for agonists versus partial agonists.

4.4.2 Interactions with serotonergic antagonists

^{3}H-granisetron interacts with B-loop residues W183, H185 and D189 on the 5-HT$_{3A}$R (Appendix 1) but little is known about how these residues interact. Two of the three residues are conserved and the third residue, D189, is substituted for another acidic residue, glutamate, on the AChBP. Given the relatively high affinity of AChBP for the antagonists granisetron, tropisetron, and MDL72222, which all contain the carbonyl oxygen from the Hibert pharmacophore, compared to lerisetron and 5-HT$_3$R agonists which do not, it is tempting to implicate interactions involving that group. However this interpretation of the data should be approached with caution since such interactions might be overshadowed by the interactions of the C-loop with agonists, and by interactions of the N-benzyl group in lerisetron, as discussed above (section 4.3.1). More detail about this interaction could be inferred using site-directed mutagenesis and possibly a broader sampling of antagonists with varied structures.

4.4.3 Location of granisetron in the 5-HT$_3$R binding site.

Joshi et al. [22] investigated the binding (docking) of granisetron to an agonist-free (lid-open) model of the 5-HT$_{3A}$R. The authors indicated two separate sets of binding sites for this molecule, and that both appear to be important; the first, "B" orientations, act as way-in sites, then "A" orientations are final resting places for granisetron (see introduction for more detail). These results are consistent with this model, since they strongly indicate a very similar

binding site for AChBP, despite the non-identical sequences of the two proteins. This is easier to explain by assuming that the residues important to binding antagonists in the 5-HT$_3$R actually make contacts with these antagonists. The Joshi model is the best one so far, since it explains the interactions with the highest number of important B-loop and other AChBP-conserved residues.

4.4.4 C- and E-loop interactions with agonists.

M-chlorophenylbiguanide (*m*CPBG), and the other agonists tested (phenylbiguanide (PBG), Serotonin (5-HT), and 2-Me-5-HT), all bind comparatively poorly to AChBP. The comparison of agonist versus antagonist data in table 4.2, taken with the degree of conservation of important residues, suggests that interactions of 5-HT with the C- and E-loops are indeed taking place in the 5-HT$_{3A}$R more than in AChBP; this strongly supports our agonist hypothesis and the models upon which it is based.

Interestingly, in comparing the partial agonist *m*CPBG to the full agonist 5-HT, the decreases in affinity of AChBP compared to 5-HT$_3$R are very different (33,000 and 1200, respectively). F226 is the only C-loop residue that is important to the binding of *m*CPBG, which is not conserved in AChBP. On the other hand, I228 and D229, in addition to F226, are both very important in binding 5-HT to the murine 5-HT$_{3A}$R. From this information we would expect *m*CPBG to be *less* specific than 5-HT to the 5-HT$_{3A}$R, and yet we find the opposite is true. The lack of interspecies conservation, and the poor alignment, of the C-loops of 5-HT$_{3A}$R's and AChBP make interpretation of this data difficult.

It has been proposed [22, 51] that the C-loop of the 5-HT$_{3A}$R and other cys-loop LGIC's forms a "lid" which closes over bound agonists- "lid shut conformation," but not antagonists- "lid open conformation." X-ray crystallography studies have shown that AChBP does adopt "lid open" and "lid shut" conformations when binding some nAChR agonists and antagonists, respectively. Further, the C-loop is known to be flexible, and has been linked in

cys-loop receptors to signal transduction (i.e. agonist-induced channel opening). Given this information, it seems likely that the AChBP C-loop adopts specific local structures, which may correspond to the conformational stability of the overall protein, and through this stability to binding affinity, when binding different serotonergic ligands.

It should be noted that it is not known which serotonergic ligands act like agonists with respect to the C-loop, and which act like antagonists on AChBP (note: "agonist" and "antagonist" are not truly proper terms here, because the AChBP is not a functional ion channel). In the future, crystal structures of serotonergic ligand-bound AChBP and energy minimization studies could be used to elucidate these structures and infer their effects on binding affinity.

4.4.5 Lerisetron binds weakly to AChBP.

The one exception to the strong-binding antagonist rule is lerisetron, a novel antagonist, which has a very high affinity for the 5-HT$_3$R, 0.8 nM Ki, [50] but a 7000-fold increase in the K$_i$ when binding to AChBP (Table 4.1 above). Mutagenesis data indicate that lerisetron interacts with Y142 and Y152 (Y143 and Y153) on the 5HT$_3$R, as do serotonergic agonists. In fact, the lerisetron-Y152 interaction is even more significant than the agonist-Y152 interaction. Alignments (figure 4.1) show that residues Y142 and Y152 are missing on AChBP. Therefore, the low affinity of lerisetron may be due to the missing interactions with Y142 and Y152 on AChBP. Lerisetron binding therefore presents an opportunity to improve on the modelling and the understanding of the binding site structure. Additionally, if Y142, Y152 and other binding site residues interact in a novel way with lerisetron, this could imply possible unique uses of lerisetron analogues as 5HT$_3$R-active drugs.

It has been proposed [52] that lerisetron binds 5HT$_3$R in a way that spans both the (partial) agonist and antagonist binding site.

4.4.6 Summary.

The acetylcholine-binding protein (AChBP) has recently been used extensively to model the N-terminal binding domains of various cys-loop ligand gated ion channels (LGIC's). There is significant sequence homology among this family of ion channels, and between their N-terminal domains and the AChBP. However, the pharmacology of the AChBP with respect to many common LGIC ligands is not well known. The focus of this work was to obtain data for binding of serotonergic ligands to the AChBP, thus checking existing serotonin type 3A homopentamer (5-HT$_{3A}$R) models. We expect a comparison between 5-HT$_{3A}$R binding affinities and AChBP binding affinities to allow evaluation and improvement of the binding models, and shed light on important differences among members of the LGIC superfamily.

We have used scintillation proximity assay to evaluate the binding of serotonin type 3 receptor (5-HT$_3$R) agonists, partial agonists and antagonists on the AChBP. These included agonists serotonin (5-HT), m-chlorophenylbiguanide (mCPBG), 2-methyl-serotonin (2-Me-5-HT), and phenylbiguanide (PBG), and antagonists lerisetron, tropisetron, granisetron and MDL72222. 5-HT$_3$R antagonists ranged from 2-30 times weaker in comparative affinity (K$_i$ on AChBP/ K$_i$ on 5-HT$_3$R), while agonists for 5-HT$_3$R had 500-30,000 times weaker binding to AChBP. Lerisetron was 7000 times weaker in binding AChBP.

Our data confirm the structural similarity of AChBP with 5-HT$_3$R and supports the validity of AChBP based antagonist and agonist binding models. Particularly, the models of binding proposed by our laboratory (Joshi et al., 2006; Suryanarayanan et al., 2005, [22, 23]) are further supported by the binding of serotonergic ligands to AChBP.

Chapter 5: Summary and Future Directions

5.1   Introduction:

In Chapter 1 of this thesis, two hypothesis were proposed: 1) The AChBP can be attached to biosensor surfaces and trigger a response that can selectively detect the presence and affinity of nicotinic ligands and 2) The AChBP can be engineered to selectively recognize different classes of LGIC by mutating key binding site amino acids in the AChBP to corresponding amino acids of the target LGIC receptor.   To test these hypotheses, and initiate development of AChBP based biosensor proteins, this thesis addressed the following 7 objectives:

1. **Develop an expression and purification scheme** for the AChBP that permits rapid purification of sufficient quantities of protein.

2. **Determine the storage qualities of the AChBP** in solution and identify ways of stably storing the protein over a long time period (months).

3. **Determine the functionality** of the receptor on three biosensor platforms – Surface Plasmon Resonance, Scintillation Proximity Assay and Microcantilevers.

4. **Determine the sensitivity and stability** of the AChBP on each of the platforms tested in Objective 3.

5. **Conduct pharmacological studies** of the AChBP to determine the affinity of a broad range of LGIC ligands with the AChBP in its native form.

6. **Construct point mutations** based on predictions from homology modelling and ligand studies of the binding domain of the serotonin type 3 receptor, which will increase affinity of serotonergic ligand and decrease affinity of nicotinic ligands (i.e. Alter the selectivity of the protein to one similar to the 5-HT$_3$R.).

7. **Using information obtained** as a result of Objective 6, create additional binding proteins aimed at mimicking selectivity of 5-HT3R subtypes.

Objectives 1-4 were addressed in chapter 3 and objective 5 was addressed in chapter 4. Objectives 6 and 7 will be discussed in this chapter and constitute future directions of this research.

5.2   Expression and purification of the AChBP.

We chose to express the AChBP in a mammalian expression system and engineered the protein for rapid affinity purification using Nickel or Anti-Flag affinity chromatography. The preferred method, due to speed and costs was Nickel affinity chromatography. Expression in HEK-293 cells was also chosen due to cost and efficiency. While both systems were highly effective at producing useable AChBP protein, both could be improved given more resources. The most reasonable addition to this procedure would be the development of a higher capacity expression system. The two best systems would likely be insect cell lines or yeast expression. Due to the ease of use and rapid production of a yeast expression system, this would likely be the best for producing large quantities of protein. However, since different expression systems can produce different proteins due to post-translational processing, these systems would likely require optimization if implemented. For the studies proposed here, large quantities of protein are not necessary and thus the HEK-293 system may remain the most productive.

The AChBP purification scheme could also be improved to provide cleaner protein. The single column approach yields remarkably pure protein (estimated at about 95%) but does contain other cellular proteins. These proteins could be eliminated by the use of a second anti-flag affinity column. We have shown in SPR studies that the AChBP binds effectively to the anti-Flag chips. This same approach can be used to create anti-Flag affinity chromatography columns. A

Nickel column followed directly by an anti-Flag column should produce protein of high purity. While unnecessary for the experiments described in this thesis, pure protein would be necessary for biophysical studies including Circular Dichroism and x-ray crystallography. Our engineered protein permits this two-step, rapid purification. The disadvantages of this approach are the moderately higher costs associated with the additional affinity media and anti-Flag antibody. As this project moves towards producing new binding proteins (objective 7 above) a more pure product will facilitate evaluation of target proteins.

5.3   The AChBP as a biosensor.

Chapter 3 also addressed the question of AChBP functionality as a biosensor protein. These studies used 3 different support media and all showed advantages and disadvantages inherent in the three platforms. The AChBP, however, performed well in all three applications, providing data consistent with published literature values and comparable across all three techniques. The differences between our data and that of the literature are modest in the perspective of the LGIC field, and are explainable by subtle differences in assay systems. Differences in between our three assay systems were not statistically significant, even though our precision was good. This confirms our hypothesis that the AChBP can be an effective biosensor protein. The data obtained in chapter 4 demonstrates the use of the AChBP in screening a series of receptor ligands.

The microcantilever data in Chapter 3 is particularly interesting since it suggests the ability of the microcantilever to detect conformational changes. As an allosteric protein, the AChBP undergoes a large conformational change when exposed to nicotinic agonists such as acetylcholine and nicotine. This change in conformation produces responses on microcantilevers greater than comparable antagonists that do not produce conformational changes. The high sensitivity of the microcantilevers was likely due to the large conformational change in the

AChBP protein. This property contributes to the success of the AChBP as a biosensor and suggests future proteins based on the AChBP could be equally good candidates for microcantilever assays.

5.4   Binding of 5-HT$_3$R receptor ligands to the AChBP.

Chapter 4 focused on obtaining useful data using one of the AChBP methods discussed in chapter 3. The goal of this study was to determine how these ligands interacted with the AChBP that has been used as a template in computer modelling studies of the 5-HT$_3$R. This is the first data showing how 5-HT$_3$R ligands bind to the AChBP and is significant in validating the 5-HT$_3$R models.

The outcome of this study is a clear difference in the binding of serotonin antagonists and agonists with the AChBP. Our initial analysis of the 5-HT$_3$R binding site suggested that, based on the current homology models of the receptor, serotonin antagonists should bind with reasonably high affinity. This hypothesis is well supported by the data. The granisetron-type antagonists bound better than expected with only slightly lower affinities on the AChBP. The similarity in binding affinities suggests that the computer models are much more likely to produce accurate depictions of the antagonist binding site. Thus this study confirms the confidence that many have placed in the quality of these models. Future mutagenesis studies (described below in section 5.5) would enable the differences between individual models to be explored in more detail. Since therapeutically, 5-HT$_3$R antagonists are presently the most important group of compounds, this data has a significant impact on drug development. Since the homology models are likely to be highly accurate, more confidence can be placed in rational drug design approaches.

Analysis of agonist binding models suggested that 5-HT$_3$R agonists would be unlikely to bind as tightly to the AChBP as they do to the 5-HT$_3$R itself. This hypothesis was also supported by our data. The differences appear to be due to

the structure of the C-loop. C-loop sequences are dramatically different and are likely to produce profound effects on receptor function in addition to ligand binding. As discussed in chapter 4, the hypothesized movement of the C-loop in response to agonist binding is thought to lead to a higher affinity binding site that is "capped" by the C-loop. This is thought to be the first step in a two-step process that leads to channel opening. Since the AChBP lacks the channel regions, this first step does not produce any effect but is necessary for high-affinity binding of agonists. The most likely explanation for the weak binding of agonists is that they bind but fail to bind well to stabilize the "lid-closed" conformation. This is supported by our data showing similar affinities for all partial and full agonists on the AChBP. Further studies of the ability of these ligands to induce a conformational change could make use of the microcantilever sensors. These sensors can detect conformational changes in proteins and are likely detecting these changes in the AChBP-modified microcantilevers described in chapter 3. Treatment of these microcantilevers with serotonin, mCPBG and PBG should produce smaller bending amplitudes when compared to acetylcholine or nicotine.

5.5   Future Directions:

This thesis addressed the first 5 of 7 objectives of a larger study. The final two objectives require modification of the AChBP based on the data obtained in chapters 3 and 4. Objective 6 is intended to produce a $5\text{-}HT_3R$ analogue based on the AChBP protein using site directed mutagenesis. This project will draw heavily on the data obtained in chapter 4 in particular. Objective 7 expands the outcome of objective 6 to produce similar binding proteins for GABA, Glycine and neuronal nicotinic receptors.

5.5.1 Developing a 5-HT$_3$R binding protein.

The goal of this future study will be to express AChBP mutants with single amino acid substitutions from equivalent positions in the 5-HT$_{3A}$R sequence, which can be synthesized and purified in quantities usable for biosensor applications. The next step in this process will be the production of mutant AChBP based on molecular modelling and previous site directed mutagenesis studies. Table 5.1 lists several primary differences between the 5-HT$_3$R and the AChBP at amino acid positions determined to interact with serotonin (see chapter 4). Several of these positions are conserved, however, some differences exist. Where amino acid composition at a specific three dimensional position is different, the AChBP amino acid can be mutated to the corresponding 5-HT$_3$R amino acid.

Mutations will be initially made singly then in groups based on the results of the single mutations. Mutations can be constructed by commercial mutagenesis services to facilitate rapid production of mutations, if funding permits, or by utilizing inexpensive oligonucleotides and Stratagene's (Cedar Creek, TX) QuickChange II site directed mutagenesis kit. Mutant receptors will then be expressed and characterized using stably transfected HEK 293 cells in a manner similar to that used to produce the wild-type AChBP (chapter 3).

Table 5.1: Proposed Mutants. The left-hand column shows the corresponding 5-HT$_{3A}$R amino acid, and the right-hand column shows the planned AChBP mutant. * denotes mutants in the region of the C-loop: the C-loops of AChBP and 5-HT$_{3A}$R don't align well, thus it may be better to replace some of these with a C-loop chimera. Note some oligonucleotides have been ordered, and we have stably expressed two of the mutants in HEK293 cells (see preliminary data in supplementary material).

Corresponding 5-HT$_{3A}$R amino acid, loop	AChBP residue/ mutation
W183, loop B	None (identical residues)
F226, loop C	V183F*
D229, loop C	S186D*
S233, loop C	A191S
Y234, loop C	None (identical residues)
E236, loop C	D194E*
E129, loop A	N90E
Y143, loop E	R104Y
Y153, loop E	M114Y
D189, loop B	E149D
Entire C loop	C-loop chimera

Recombinant proteins will be purified using affinity chromatography (Sigma His-select columns, chapter 2) and characterized using immunoblotting and SDS-PAGE (denaturing and non-denaturing) analysis. To determine integrity of quaternary structure, we will employ gel exclusion analysis and non-denaturing PAGE assay. Functional properties will be determined by saturation as well as competition ligand binding assays. Mutant binding proteins will initially be evaluated by Scintillation Proximity Assay (SPA) or Surface plasmon resonance (SPR) then attached to microcantilever surfaces for further testing. SPR will be helpful in evaluating the engineered proteins as potential biosensor molecules.

5.5.2 Development of other LGIC Binding proteins.

Each of the well-known families of cys-loop LGIC's, GABA type A and C (GABA$_A$R, GABA$_C$R), Glycine (GlyR), serotonin type 3 receptors, (5-HT$_3$R), and nicotinic acetylcholine receptors (nAChR) have now been modelled based on the AChBP [22, 30, 31, 48, 53-57]. These models have brought together a considerable amount of useful information on binding site structure for the LGIC receptor superfamily. A long term goal of the research initiated in this thesis will be to develop an equivalent superfamily of binding proteins that can be used in place of the membrane bound receptor proteins. The advantages of soluble proteins have been discussed earlier but include ease of purification, storage and immobilization on biosensor devices. A complete selection of these proteins would enable extremely fast evaluation of new drugs but would also permit devices designed to detect endogenous ligands in brain or other tissues. To obtain these proteins, accurate homology models must be constructed. This section describes current receptor models for GABA$_A$, GABA$_C$ and Glycine receptors that will be the initial targets of future binding protein development.

5.5.2.1 GABA$_A$R Models.

GABA$_A$R are inhibitory chloride channels which are central to the action of general anaesthetics, barbiturates, alcohol, and benzodiazepines. AChBP (*Lymnaea stagnalis*, PDB file 1I9B) was recently used to model the ligand-binding domain (LBD) of these LGIC's [28, 30, 58]. The researchers noted that there are an unequal number of amino acids in a few relevant areas of the primary sequence of the GABA$_A$R compared to the AChBP; consequently, the alignments, and therefore the structural and functional homology is to be viewed with caution. The GABA$_A$R receptor LBD sequence allows for a likely "modified globulin-like" structure consisting of an N-terminal α-helix followed by ten β-strands intercalated by ten loop structures and two short "3-10" helices. Binding "loops" (or segments) A-F have been defined [58], as in nAChR and 5-HT$_3$R

(chapters 1, 4), and again a "+" and "-" face can be defined and are contributed by loops A-C and D-F, respectively. As with heteromeric nAChR's, one subtype (β) contributes the "+" face and another (α) contributes the "-" face to the binding site (in the nAChR, the α-β naming is the opposite, since the naming of the subunits preceded an understanding of the binding sites). Each of the AChBP models below verifies this structural information, in addition to providing information on the individual binding residues.

The First AChBP GABA$_A$R modelling was performed by in 2002 by Cromer et al. [58]. They modelled the most prevalent GABA$_A$R in the human brain, the α1β2γ2 receptor, which data indicate are -β2-α1-β2-α1-γ2- hetero-pentamers, with GABA-binding sites at the two β2-α1 plus-minus interfaces, and a benzodiazepine-binding site at the α1-γ2 interface. The binding pocket in this model is surrounded by a "box" of aromatic residues, which is similar to the aromatic residues said to have cation–π interactions with nicotinic agonists in nAChR and the quaternary ammonium of N-2-hydroxyethylpiperazine-N9-2-ethanesulphonic acid (HEPES) in the AChBP structure [27, 59]. This box consists of the aromatic residues β2 F200, Y205 (β2 loop C) Y157 (β2 loop B), and F65 (α1 loop D). R67 (α1 loop D), and maybe R132 (α1 loop E) interact with the carboxy moiety of GABA. R120 (α1 loop E), surrounding residues such as Tyr205, T202, R207, (β2 loop C), and T160 (β2 loop B) may also be important in this model, but the authors did not specifically indicate what interactions these residues might have. In addition to the LBD, these authors also speculated on the benzodiazepine-binding site and the signal transduction mechanism.

Ernst et al. also modelled the GABA$_A$R ligand binding domain [28] based on AChBP, and provide a detailed and lucid account of the problems inherent in such a model. These researchers preferred the term "comparative" rather than homology modelling, based, among other things, on their estimate that only 60-75% of GABA$_A$R residues have structural homologues ("equivalents") in AChBP. It seems, therefore that AChBP chimeras, which could incorporate GABA-binding

sequences, thus increasing homology may be a necessary step in the validation of these models.

A GABA$_A$R model was recently made using "quasi-ab-initio" methods for modelling the positions of the putative GABA binding loops [30]. The model was made to agree with known data: F65, R67, S69 ("loop D"), R120, I121 ("loop E"), R177, V179, V181 and E184 ("loop F") from the α1 subunit, and Y97, L99 ("loop" A), Y157, T160 ("loop B"), T202, S204, Y205, R207 and S209 ("loop C") from the β2 subunit are found to be located in the GABA binding pocket.

This could be an oversight, but it seems that GABA$_A$R models have so far not had their predictive value tested. It is the opinion of this author that such testing could be done easily on AChBP, and with great affect on chimaeric AChBP's (i.e. AChBP-based GABA-binding proteins).

5.5.2.2 GABA$_C$R model.

Modeling of the GABA$_C$R, also called the Rho receptor, specifically the ρ1 homopentamer, was performed by Harrison et al [31]. Emerging from this study is a binding site where tyrosine residues play an important role; when GABA is docked to this model, tyrosines from loops D (Y102), E (Y167), B (Y198), and C (Y241, Y247) are within 5 Å of GABA in energetically favorable orientations. Other residues close to GABA are also in the expected binding loops, notably, R104 in loop D, S168 (loop E), and S243 (loop C). Three energetically favorable orientations are discussed, all of which have Y198, S168, and S243 within 5 Å of GABA. In the first, the amine group of GABA is directed into a pocket formed by loop E (- face), where it hydrogen bonds with two backbone carbonyls (of M156 and L166), and the hydroxyl of S168; meanwhile the carboxyl group of GABA projects toward the C-loop and B-loop of the + face, where it fails to make convincing contacts. A, D, and F-loop contacts are absent in the first orientation, only two C-loop residues are within 5 Å, and the hydrogen bonding capability of GABA's carboxy moiety seems not fully utilized.

In the second orientation, the GABA molecule is flipped endwise and shifted closer to the C-loop and B-loop by 3 Å, putting C-loop residue Y241, A-loop's F138, and D-loop's Y102 within cation-π interaction range of GABA's amine. However, in the E-loop, only S168 is within 5 Å of GABA, and with Y198 (B-loop), is one of the two residues that might hydrogen bond (if weakly) to the carboxyl end of GABA. The third orientation, "Harrison orientation 3," is the favorite. The carboxylate end of GABA is close to the basic R104, H105 residues of the D-loop, so they would stabilize that group. In loop E, the important S168 residue oxygen and the backbone of L166 can hydrogen bond with the amine group. Finally, important B-loop residue Y198 could make a cation-π interaction with the amine. The C-loop is mostly left out of this model; however the modelers did not allow the residues to move upon ligand binding, so there is clearly some room to improve the modeling in this flexible area (the authors mention this general flaw in their modeling, but don't relate it specifically to the C-loop).

Interestingly, considered in terms of the theory that the C-loop is largely responsible for LGIC subunit specificity, the lack of involvement of the C-loop could be key to the differences between the GABA$_A$R and GABA$_C$R relating to antagonist binding (bicuculine) and putative lack of desensitization in GABA$_C$R's. Regarding another point more directly relevant to the topic of this thesis, the modelers do not seem to consider the fact, in their model, that their template AChBP does not bind GABA [3]. Harrison "orientation 3" [31] is consistent with that fact, in that AChBP's D-loop contains no positively charged residues; thus an area where an AChBP mutant might be of value. In another possibly key position, AChBP's E-loop M114 aligns with GABA$_C$R S168 – methionine would not effectively hydrogen bond with GABA's amine. The importance, which the modelers of GABA A and C receptors stress, of aromatic residues in the binding site, may well be great, but it certainly does not explain why GABA does not bind to AChBP, since residues in aromatic positions in GABA$_A$R's and GABA$_C$R's are

either identical residues in AChBP, or are replaced by tryptophan, which should be even more effective.

5.5.2.3 GlyR model.

The GlyR α1 homopentamer was modelled using AChBP by Speranskiy et al [54]. One advantage of this model was that the authors had the foresight to use an alignment that utilized the *Aplysia* as well as *Lymnaea* AChBP. The overall structural conformation of the glycine LBD in this model is similar to the AChBP's LBD. Docking studies were done using the GlyR antagonist strychnine, and it was recognised that other docking studies are needed. However, it is apparent that strychnine, at least, binds in the usual pocket, more or less deep to, and membrane-side of, the C-loop (naming of the loops in this paper follows Brejc et al's AChBP naming [27] and can be compared using figure 4.1 of chapter 4). Several C-loop residues are close to strychnine, as well as two E-loop residues and an F-loop residue. Instead of B-loop residues being involved as with other cys-loop LGIC's, two residues membrane-side of the A-loop appear close to strychnine. Specific interactions are not explored. It should be noted that strychnine is much larger than glycine, and thus may not relate in the same way to the flexible C-loop; for instance, the antagonist could act more by blocking entry into, rather than occupying the agonist-binding site. Mutations to the AChBP, as well as comparative studies of the GlyR-related pharmacology of the two AChBP's should again be useful here; however, more modelling and/or docking studies will be needed in order to make progress.

5.6. Further Pharmacological testing of AChBP.

GABA type A and Glycine (GlyR) receptors have recently been modelled based, in part, on the AChBP (section 5.5). However, with the exception of GABA and glycine themselves, which did not bind to the AChBP, none of the ligands associated with these receptors have been characterized with respect to their

binding to AChBP. Besides these models, several models of both homo- and heteromeric nAChR's and 5-HT$_3$R's depend on AChBP. A broad range of nAChR compounds and now several 5-HT$_3$R ligands (see chapter 4) have been tested on AChBP, which have already added to the validity of those models. However, there is potential to learn more about sites other than the primary binding sites for these receptors from the AChBP. Thus, in addition to GABAR and GlyR ligands, nAChR allosteric ligands also need to be studied using the AChBP. Table 5.2 shows some compounds which should be tested on AChBP in order to further characterize AChBP's pharmacology.

Table 5.2. Compounds to be tested on AChBP. By no means is this a complete list. *Tropisetron is a GlyR potentiator [2], and it would be interesting to know why, and if the binding site is the same as on AChBP.

Compounds that should be tested on AChBP		
Peptides	SLURP1, SLURP2, galanin gephyrin	
Heavy metals		
nAChR potentiators	azieomidate, etomidate, phencyclidine	
Divalent cations of Ca, Zn, Cu, Cd, Ni, Mn, Co		
Barbiturates	Thiopental, MPPB, TID, barbital, pento-, amyl-, seco-, and iso- barbital,	Act on nAChR's as well as GABA$_A$R's and likely others
SSRI's	Flouxetine	
TCA's	Imipramine	
SNRI's and NSRI's	Venlaflaxine	
So called non-competitive nAChR antagonists	Quinacrine, Tetracaine, dizocilpine, phencyclidine, ketamine	
Allosteric nAChR modulators	Galanthamine, Physostigmine, dFBr and analogues, ryanodine	
Tabacco alkaloids, nicotine metabolites		See Arneric and Brioni, 1999, pg 214-218
GABAaR competitive antagonists	Bicuculine, gabazine,	
GABAaR competitive agonists	Muscimol	
Benzodiazpines	Flunitrazapam, diazepam. Zolpidem	Classic GABA$_A$R allosteric modulators
GABAcR agonist/ partial agonist and antagonist ligands	3-APMPA, TPMPA, Imidazole-4-acetic acid, picrotoxin, CACA, TACA, isoguvacine	
Neurosteriods	THPROG, pregnalone, dehydropiandrosterone	
Anaesthetics		Act on GABA, other receptors
Ginko biloba compounds		Act on glycine receptors
GlyR potentiators	Ethanol, and other n-alcohols, propofol, *	

5.7. General Summary.

Ligand-Gated Ion Channels like the serotonin 5-HT$_3$R are involved in a wide range of physiological processes including nerve conduction, regulation of blood flow, fluid balance and gastric motility. In the central nervous system, these important proteins mediate fast excitatory and inhibitory neurotransmission. The construction of a serotonin binding protein would enable the development of a molecular biosensor for serotonin. Chapter 3 explored the potential of the AChBP as a biosensor, and chapter 4 establishes a baseline from which to evaluate serotonergic AChBP mutants. Although the project has not yet reached the point of a viable serotonin biosensor, the previous chapters lay the groundwork for future studies as described in section 5.5 above.

This project is highly significant and contributes to human health. In addition to drug development applications sensors of this type could be used for in-vivo, in-vitro and environmental biosensor applications. The data presented in this thesis provide a firm foundation on which to build a family of biosensor proteins covering the spectrum of LGIC receptors.

References

1. Nelson DL, Cox, MM: **Lehninger Principles of Biochemistry, 4th ed.** New York: W. H. Freeman and Company; 2005.

2. Arias HR, Ed.: **Biological and Biophysical Aspects of Ligand-Gated Ion Channel Receptor Superfamilies.** Kerala, India: Research Signpost; 2006.

3. Smit AB, Syed NI, Schaap D, van Minnen J, Klumperman J, Kits KS, Lodder H, van der Schors RC, van Elk R, Sorgedrager B *et al.* **A glia-derived acetylcholine-binding protein that modulates synaptic transmission.** *Nature* 2001, **411**(6835):261-268.

4. Hogg RC, Raggenbass M, Bertrand D: **Nicotinic acetylcholine receptors: from structure to brain function.** *Rev Physiol Biochem Pharmacol* 2003, **147**:1-46.

5. Unwin N: **Refined structure of the nicotinic acetylcholine receptor at 4A resolution.** *J Mol Biol* 2005, **346**(4):967-989.

6. Levin ED, Rezvani AH: **Nicotinic treatment for cognitive dysfunction.** *Curr Drug Targets CNS Neurol Disord* 2002, **1**(4):423-431.

7. Maelicke A, Schrattenholz A, Samochocki M, Radina M, Albuquerque EX: **Allosterically potentiating ligands of nicotinic receptors as a treatment strategy for Alzheimer's disease.** *Behav Brain Res* 2000, **113**(1-2):199-206.

8. Guan ZZ, Zhang X, Ravid R, Nordberg A: **Decreased protein levels of nicotinic receptor subunits in the hippocampus and temporal cortex of patients with Alzheimer's disease.** *J Neurochem* 2000, **74**(1):237-243.

9. Lippiello PM: **Nicotinic cholinergic antagonists: a novel approach for the treatment of autism.** *Med Hypotheses* 2006, **66**(5):985-990.

10. Diehl A, Nakovics H, Croissant B, Smolka MN, Batra A, Mann K: **Galantamine reduces smoking in alcohol-dependent patients: a randomized, placebo-controlled trial.** *Int J Clin Pharmacol Ther* 2006, **44**(12):614-622.

11. Gaddum JH, Picarelli ZP: **Two kinds of tryptamine receptor.** *Br J Pharmacol Chemother* 1957, **12**(3):323-328.

12. Derkach V, Surprenant A, North RA: **5-HT3 receptors are membrane ion channels.** *Nature* 1989, **339**(6227):706-709.

13. Reeves DC, Lummis SC: **The molecular basis of the structure and function of the 5-HT3 receptor: a model ligand-gated ion channel (review).** *Mol Membr Biol* 2002, **19**(1):11-26.

14. Niesler B, Walstab J, Combrink S, Moller D, Kapeller J, Rietdorf J, Bonisch H, Gothert M, Rappold G, Bruss M: **Characterization of the novel human serotonin receptor subunits 5-HT3C,5-HT3D, and 5-HT3E.** *Mol Pharmacol* 2007, **72**(1):8-17.

15. Bonhaus DW, Wong EH, Stefanich E, Kunysz EA, Eglen RM: **Pharmacological characterization of 5-hydroxytryptamine3 receptors in murine brain and ileum using the novel radioligand [3H]RS-42358-197: evidence for receptor heterogeneity.** *J Neurochem* 1993, **61**(5):1927-1932.

16. Dubin AE, Huvar R, D'Andrea MR, Pyati J, Zhu JY, Joy KC, Wilson SJ, Galindo JE, Glass CA, Luo L *et al*: **The pharmacological and functional characteristics of the serotonin 5-HT(3A) receptor are specifically modified by a 5-HT(3B) receptor subunit.** *J Biol Chem* 1999, **274**(43):30799-30810.

17. Das P, Dillon GH: **The 5-HT3B subunit confers reduced sensitivity to picrotoxin when co-expressed with the 5-HT3A receptor.** *Brain Res Mol Brain Res* 2003, **119**(2):207-212.

18. van Hooft JA, Yakel JL: **5-HT3 receptors in the CNS: 3B or not 3B?** *Trends Pharmacol Sci* 2003, **24**(4):157-160.

19. Brady CA, Dover TJ, Massoura AN, Princivalle AP, Hope AG, Barnes NM: **Identification of 5-HT3A and 5-HT3B receptor subunits in human hippocampus.** *Neuropharmacology* 2007, **52**(5):1284-1290.

20. Tzvetkov MV, Meineke C, Oetjen E, Hirsch-Ernst K, Brockmoller J: **Tissue-specific alternative promoters of the serotonin receptor gene HTR3B in human brain and intestine.** *Gene* 2007, **386**(1-2):52-62.

21. Schulte MK, Hill RA, Bikadi Z, Maksay G, Parihar HS, Joshi P, Suryanarayanan A: **The Structural Basis of Ligand Interactions in the 5-HT3 Receptor Binding Site.** In: *Biophysical Aspects of Ligand-Gated Ion Channel Receptor Superfamilies.* Edited by Arias HR. Trivandrum, India: Research Signpost; 2005.

22. Joshi PR, Suryanarayanan A, Hazai E, Schulte MK, Maksay G, Bikadi Z: **Interactions of granisetron with an agonist-free 5-HT3A receptor model.** *Biochemistry* 2006, **45**(4):1099-1105.

23. Suryanarayanan A, Joshi PR, Bikadi Z, Mani M, Kulkarni TR, Gaines C, Schulte MK: **The loop C region of the murine 5-HT3A receptor contributes to the differential actions of 5-hydroxytryptamine and m-chlorophenylbiguanide.** *Biochemistry* 2005, **44**(25):9140-9149.

24. Joshi PR, Suryanarayanan A, Bikadi Z, Schulte MK: **Mutations at loop E tyrosine residues differentially modulate gating of the murine 5-HT₃A receptor.** In: *Society for Neuroscience Abstracts 2004; New Orleans, LA*: Society for Neuroscience; 2004: 626.622.

25. Hansen SB, Talley TT, Radic Z, Taylor P: **Structural and ligand recognition characteristics of an acetylcholine-binding protein from Aplysia californica.** *J Biol Chem* 2004, **279**(23):24197-24202.

26. Celie PH, Klaassen RV, van Rossum-Fikkert SE, van Elk R, van Nierop P, Smit AB, Sixma TK: **Crystal structure of acetylcholine-binding protein from Bulinus truncatus reveals the conserved structural scaffold and sites of variation in nicotinic acetylcholine receptors.** *J Biol Chem* 2005, **280**(28):26457-26466.

27. Brejc K, van Dijk WJ, Klaassen RV, Schuurmans M, van Der Oost J, Smit AB, Sixma TK: **Crystal structure of an ACh-binding protein reveals the ligand-binding domain of nicotinic receptors.** *Nature* 2001, **411**(6835):269-276.

28. Ernst M, Brauchart D, Boresch S, Sieghart W: **Comparative modeling of GABA(A) receptors: limits, insights, future developments.** *Neuroscience* 2003, **119**(4):933-943.

29. Costa V, Nistri A, Cavalli A, Carloni P: **A structural model of agonist binding to the alpha3beta4 neuronal nicotinic receptor.** *Br J Pharmacol* 2003, **140**(5):921-931.

30. Campagna-Slater V, Weaver DF: **Molecular modelling of the GABAA ion channel protein.** *J Mol Graph Model* 2007, **25**(5):721-730.

31. Harrison NJ, Lummis SC: **Molecular modeling of the GABA(C) receptor ligand-binding domain.** *J Mol Model* 2006, **12**(3):317-324.

32. Reeves DC, Sayed MF, Chau PL, Price KL, Lummis SC: **Prediction of 5-HT3 receptor agonist-binding residues using homology modeling.** *Biophys J* 2003, **84**(4):2338-2344.

33. Thompson AJ, Padgett CL, Lummis SC: **Mutagenesis and molecular modeling reveal the importance of the 5-HT3 receptor F-loop.** *J Biol Chem* 2006, **281**(24):16576-16582.

34. Biacore: **Technology Note 1 BR 9001-15 2001.** In., BR 9001-15 2001edn: Biacore AB; 2001.

35. Gao H, Buchapudi KR, Harms-Smyth A, Schulte MK, Xu X, Ji HF: **Improved Surface Modification Approach for Micromechanical Biosensors**. *Langmuir* 2007.

36. Turbadar T: **Complete Absorption of Light by Thin Metal Films**. *Proceedings of the Physical Society* 1959, **73**(1):40-44.

37. Zhang Y, Ji HF, Brown GM, Thundat T: **Detection of CrO4(2-) using a hydrogel swelling microcantilever sensor**. *Anal Chem* 2003, **75**(18):4773-4777.

38. Fritz J BM, Lang HP, Rothuizen H, Vettiger P, Meyer E, Guntherodt H--J, Gerber G, Gimzewski JK: **Translating Biomolecular Recognition into Nanomechanics**. *Science* 2000, **288**:316-318.

39. Butt H-J: **A Sensitive Method to Measure Changes in the Surface Stress of Solids**. *Journal of Colloid and Interface Science* 1996, **180**(1):251-260.

40. Thundat T, Warmack RJ, Chen GY, Allison DP: **Thermal and ambient-induced deflections of scanning force microscope cantilevers**. *Applied Physics Letters* 1994, **64**(21):2894-2896.

41. Ji H-F, Dabestani R, Brown GM, Britt, PF: **A novel self-assembled monolayer (SAM) coated microcantilever for low level caesium detection**. *Chemical Communications* 2000, **2000**(6):457-458.

42. Hansen SB, Radic Z, Talley TT, Molles BE, Deerinck T, Tsigelny I, Taylor P: **Tryptophan fluorescence reveals conformational changes in the acetylcholine binding protein**. *J Biol Chem* 2002, **277**(44):41299-41302.

43. Johnsson B, Lofas, S and Lindquist, G. : **Immobilization of proteins to a carboxymethyidextran-modified gold surface for biospecific interaction analysis in surface plasmon resonance sensors**. *Anal Biochem* 1991, **198**:268-277

44. Velanki S, Ji H-F: **Detection of feline coronavirus using microcantilever sensors**. *Measurement Science and Technology* 2006, **17**(11):2964-2968.

45. Wang H, Chen S, Li L, Jiang S: **Improved Method for the Preparation of Carboxylic Acid and Amine Terminated Self-Assembled Monolayers of Alkanethiolates**. *Langmuir* 2005, **21**(7):2633-2636.

46. Hansen SB, Taylor P: **Galanthamine and non-competitive inhibitor binding to ACh-binding protein: evidence for a binding site on non-alpha-subunit interfaces of heteromeric neuronal nicotinic receptors**. *J Mol Biol* 2007, **369**(4):895-901.

47. Joshi PR: **Structure-function studies of the serotonin type-3 receptor ligand-binding domain**. Fairbanks, AK: University of Alaska, Fairbanks; 2005.

48. Maksay G, Bikadi Z, Simonyi M: **Binding interactions of antagonists with 5-hydroxytryptamine3A receptor models.** *J Recept Signal Transduct Res* 2003, **23**(2-3):255-270.

49. Thompson AJ, Price KL, Reeves DC, Chan SL, Chau PL, Lummis SC: **Locating an antagonist in the 5-HT3 receptor binding site using modeling and radioligand binding.** *J Biol Chem* 2005, **280**(21):20476-20482.

50. Venkataraman P, Venkatachalan SP, Joshi PR, Muthalagi M, Schulte MK: **Identification of critical residues in loop E in the 5-HT3ASR binding site.** *BMC Biochem* 2002, **3**:15.

51. Karlin A: **Emerging structure of the nicotinic acetylcholine receptors.** *Nat Rev Neurosci* 2002, **3**(2):102-114.

52. Parihar HS, Suryanarayanan A, Ma C, Joshi P, Venkataraman P, Schulte MK, Kirschbaum KS: **5-HT(3)R binding of lerisetron: an interdisciplinary approach to drug-Receptor interactions.** *Bioorg Med Chem Lett* 2001, **11**(16):2133-2136.

53. Le Novere N, Grutter T, Changeux JP: **Models of the extracellular domain of the nicotinic receptors and of agonist- and Ca2+-binding sites.** *Proc Natl Acad Sci U S A* 2002, **99**(5):3210-3215.

54. Speranskiy K, Cascio M, Kurnikova M: **Homology modeling and molecular dynamics simulations of the glycine receptor ligand binding domain.** *Proteins* 2007, **67**(4):950-960.

55. Maksay G, Simonyi M, Bikadi Z: **Subunit rotation models activation of serotonin 5-HT3AB receptors by agonists.** *J Comput Aided Mol Des* 2004, **18**(10):651-664.

56. Mordvintsev DY, Polyak YL, Kuzmine DA, Levtsova OV, Tourleigh YV, Kasheverov IE: **A model for short alpha-neurotoxin bound to nicotinic acetylcholine receptor from Torpedo californica.** *J Mol Neurosci* 2006, **30**(1-2):71-72.

57. Sine SM, Wang HL, Gao F: **Toward atomic-scale understanding of ligand recognition in the muscle nicotinic receptor.** *Curr Med Chem* 2004, **11**(5):559-567.

58. Cromer BA, Morton CJ, Parker MW: **Anxiety over GABA(A) receptor structure relieved by AChBP.** *Trends Biochem Sci* 2002, **27**(6):280-287.

59. Zhong W, Gallivan JP, Zhang Y, Li L, Lester HA, Dougherty DA: **From ab initio quantum mechanics to molecular neurobiology: a cation-pi binding site in the nicotinic receptor.** Proc Natl Acad Sci U S A 1998, 95(21):12088-12093.